Diagnostic Methodologies for Generic Differential Pressure Flow Meters

By Richard Steven, DP Diagnostics LLC, PO Box 121, Windsor, CO 80550-0121

1. Introduction

There is increasing demand for flow meters with lower uncertainty and for flow meters capable of self diagnosing problems. Marginal reductions in flow meter uncertainty are important, but a stated meter uncertainty is only truly meaningful when there is a guarantee the meter is operating correctly.

Flow meters typically give the primary pipe flow rate reading, as when a flow rate is otherwise known there is little requirement for a flow meter. Therefore, often an engineer is only capable of deducing that a meter has a problem when there is a substantial discrepancy between the expected and meter predicted flows. If a meter is in error by only a few percent it may not be noticeable. Even if a piping systems mass balance shows a discrepancy, it can be difficult to confirm that a particular meter is in error. Furthermore, it is usually an order of magnitude more difficult again, to spot a small or moderate flow meter error if no potential error is indicated from external sources.

Flow meter verification is becoming as important an aspect of flow metering as the uncertainty of a meter working flawlessly. A useful tool for any flow meter is the ability to self diagnose its performance and immediately indicate any problem. A main flow metering technology is the generic Differential Pressure (DP) meter[1]. The DP meter uses pressure, temperature and DP transmitters to take primary readings. Transmitters supply information to flow computers or flow computers can be combined with transmitters to make "smart" transmitters. Flow computers calculate the flow rate. Some smart transmitters have limited diagnostic abilities to monitor individual raw input signals. However, while DP meters are seen as relatively inexpensive, rugged, trusted and reliable, they do not have any universally accepted self diagnostic capabilities. There is often a "plug and pray" mentality to DP meters, based on their good track record and an inherent acceptance that there is no diagnostic capability available.

In this paper the fluid mechanic phenomena associated with DP meters are reviewed and system redundancy factors are discussed. A DP meter diagnostic methodology is developed based on fundamental hydraulic pipe theory. Finally, practical examples with test data are presented to show the practicality and limitations of such a diagnostic methodology.

2. Fundamental Fluid Mechanics Associated with Generic Differential Pressure Flow Meters

A DP meter uses a geometric constriction to produce momentum change in a flow. Applying mass and energy conservation equations between pipe cross sections upstream and in the vicinity of the constriction produces a flow rate equation dependent on geometry, fluid density and DP. However, a geometric expansion can be used instead, as implied by Fox & McDonald [1] and later explicitly stated by Steven [2].

2.a Derivation of the Generic Constriction DP Meter Flow Equation

Consider incompressible, horizontal, reversible flow through a DP meter as shown in Fig 1. (A Venturi is shown here but any DP meter geometry would have worked, including those that allow uncontrolled contraction and / or expansion of the flow area, e.g. orifice plate meters.)

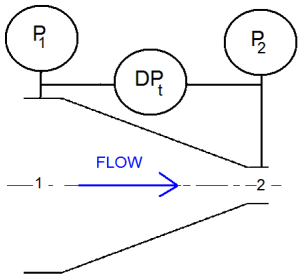

Fig 1. Generalised Constriction DP Meter

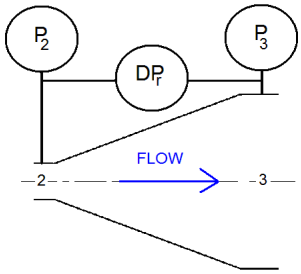

Fig 2. Generalised Expansion DP Meter

Mass continuity and energy conservation gives Equations 1 and 2 respectively:

[1] In this paper the term "DP meter" does not include the special case of laminar flow element devices.

$$\dot{m} = \rho \dot{Q} = \rho A_1 U_1 = \rho A_2 U_2 \quad \text{--- (1)} \quad \text{and} \quad \frac{P_1}{\rho} + \frac{U_1^2}{2} = \frac{P_2}{\rho} + \frac{U_2^2}{2} \quad \text{--- (2)}$$

where $\dot{m}$ is the mass flow rate, $\dot{Q}$ the volume flow rate, A_1 & A_2 are the inlet and outlet areas respectively, P_1 & P_2 are the inlet and outlet pressures respectively, U_1 & U_2 are the inlet and outlet average velocities respectively and ρ is the density. Let the beta ratio, β, be defined by equation 3, therefore:

$$\beta = \sqrt{\frac{A_2}{A_1}} \text{ --(3)}, \quad \frac{P_1 - P_2}{\rho} = \frac{U_2^2 - U_1^2}{2} = \frac{U_2^2}{2}\left(1 - \left(\frac{U_1^2}{U_2^2}\right)\right) = \frac{U_2^2}{2}\left(1 - \left(\frac{A_2}{A_1}\right)^2\right) = \frac{U_2^2}{2}\left(1 - \beta^4\right) \text{ --(2a)}$$

E (the velocity of approach) is defined by equation 4. Therefore:

$$E = \frac{1}{\sqrt{1-\beta^4}} \text{ --- (4)} \quad , \quad U_2 = \sqrt{\frac{2(P_1 - P_2)}{\rho(1-\beta^4)}} = E\sqrt{\frac{2(P_1 - P_2)}{\rho}} \text{ ---- (2b)}$$

Substituting equation 2b into equation 1 gives:

$$\dot{m} = \rho A_2 U_2 = E A_2 \sqrt{2\rho(P_1 - P_2)} \text{ ---- (5)}$$

2.b Derivation of a Generic Expansion DP Meter Flow Equation

The same physical laws apply for incompressible, horizontal, reversible flow through a meter geometry shown in Figure 2:

$$\dot{m} = \rho \dot{Q} = \rho A_2 U_2 = \rho A_3 U_3 \quad \text{--- (1a)} \quad \text{and} \quad \frac{P_2}{\rho} + \frac{U_2^2}{2} = \frac{P_3}{\rho} + \frac{U_3^2}{2} \quad \text{--- (2c)}$$

Let the expansion beta ratio, β', be defined by equation 3a and re-arrange equation 2c to get equation 2d:

$$\beta' = \sqrt{\frac{A_2}{A_3}} \text{ -(3a)}, \frac{P_3 - P_2}{\rho} = \frac{U_2^2 - U_3^2}{2} = \frac{U_2^2}{2}\left(1 - \left(\frac{U_3^2}{U_2^2}\right)\right) = \frac{U_2^2}{2}\left(1 - \left(\frac{A_2}{A_3}\right)^2\right) = \frac{U_2^2}{2}\left(1 - \beta'^4\right) \text{-(2d)}$$

E' (the velocity of departure) is defined by equation 4a. Substitute this into equation 2d and re-arrange:

$$E' = \frac{1}{\sqrt{1-\beta'^4}} \text{ --- (4a)} \quad , \quad U_2 = \sqrt{\frac{2(P_3 - P_2)}{\rho(1-\beta'^4)}} = E'\sqrt{\frac{2(P_3 - P_2)}{\rho}} \text{ --- (2e)}$$

Substituting equation 2e into equation 1 gives:

$$\dot{m} = \rho A_2 U_2 = E' A_2 \sqrt{2\rho(P_3 - P_2)} \text{ ---- (6)}$$

2.c. Comparisons of the Classic Constriction and Expansion Type Generic DP Meters

The analysis assumed reversible flow through two conduits that are mirror images, i.e. they are geometrically symmetrical. Therefore, Equations 5 and 6 are mirror images as the considered flow through Figure 2 is precisely the flow through Figure 1 in reverse. In reality flows are irreversible so DP meters have corrections factors. A constriction DP meter flow coefficient, K, is defined by equation 7. This accounts of all factors not accounted for by theory. Note that for gas flows, density changes with the pressure and hence an incompressible flow assumption is not valid. The contraction DP meters density correction is called the expansibility, ε. This is some function f_1 (see equation 8). If the expansibility effect is known it can be separated from the flow coefficient. The discharge coefficient (C_d) is a correction factor that accounts for the remaining factors.

$$K = C_d \varepsilon = \frac{\dot{m}}{\dot{m}_{,theoretical}} = \frac{\dot{m}}{EA_2\sqrt{2\rho\Delta P_t}} \text{ --- (7) and } \varepsilon = f_1\left(P_1, \Delta P_t, \kappa, \beta\right) \text{ --- (8)}$$

Note $\dot{m}$ is the actual mass flow rate, $\dot{m}_{g,theoretical}$ is the value predicted by equation 5, κ is the gases isentropic exponent and $\Delta P_t = P_1 - P_2$. If a flow is incompressible the expansibility is unity. From theory, for a constriction DP meter, C_d <1 and $\varepsilon \le 1$ (see Appendix). Therefore K < 1. We now have:

$$\dot{m} = EA_2\varepsilon C_d\sqrt{2\rho\left(P_1 - P_2\right)} = EA_2 K\sqrt{2\rho\Delta P_t} \text{ --- (5a) where } K = \varepsilon C_d \text{ --- (9)}$$

If the expansibility has been derived for a set constriction DP meter it is typical to calibrate the meter by use of the discharge coefficient. If no expansibility has been derived the meter is calibrated by use of the flow coefficient. A simple methodology is to set a constant value for the coefficient in use. However, it is sometimes necessary to fit the coefficient to the Reynolds number to get a higher precision flow meter. The Reynolds number is shown in equation 10, and the data fits to the coefficients in equations 11 and 11a:

$$\text{Re} = \frac{inertia\ \ forces}{viscous\ \ forces} = \frac{4\dot{m}}{\pi\mu D} \text{ --- (10)}, \quad K = f_2\left(\text{Re}\right) \text{ --- (11) or } C_d = f_3\left(\text{Re}\right) \text{ --- (11a)}$$

where μ is the viscosity, D is a length (e.g. meter inlet diameter) and functions f_2 & f_3 are meter dependent data fit functions. In this case the mass flow rate is calculated by iterating equation 5a.

An expansion meter would have an "expansion flow coefficient", K_r (equation 7a). An expansion slows a gas flow, increasing the pressure and density. A compression factor (ε') could account for this phenomenon (see equation 8a, where f_4 is some particular function). If the flow is incompressible the compression factor is unity. Note that here $\dot{m}_{,theoretical}$ is the value predicted by equation 6 and $\Delta P_r = P_3 - P_2$.

$$K_r = \varepsilon' C_d' = \frac{\dot{m}}{\dot{m}_{,theoretical}} = \frac{\dot{m}}{E' A_2\sqrt{2\rho\left(P_3 - P_2\right)}} \text{ -- (7a) and } \varepsilon' = f_4\left(P_2, \Delta P_r, \kappa, \beta'\right) \text{ -- (8a)}$$

If a compression factor was known, the expansion flow coefficient (K_r) could be split into the two components of the compression factor (ε') and the expansion discharge coefficient (C_d'), which would account for the remaining factors. The expansion discharge coefficient can be greater or less than unity and $\varepsilon' \ge 1$. Therefore, unlike the flow coefficient, K, the expansion flow coefficient K_r (equation 7a) could be greater or less than unity (see Appendix). When including the expansion flow coefficient in the derived expansion DP meter equation we get:

$$\dot{m} = E' A_2 C_d' \varepsilon'\sqrt{2\rho\left(P_3 - P_2\right)} = E' A_2 K_r\sqrt{2\rho\Delta P_r} \text{ --- (6a) as } K_r = \varepsilon' C_d' \text{ --- (9a)}$$

With no compression factor currently available for expansion DP meters practical calibrations would use the expansion flow coefficient. It would depend on the expansion flow coefficient sensitivity to Reynolds number whether a constant value or a function of the Reynolds number, $K_r = f_4\left(\text{Re}\right)$, should be used.

2.d. General Hydraulic Pipe Flow Theory and Metering by Permanent Pressure Loss

The permanent pressure loss, or "PPL" (h_{lm}), across any intrusive component in a pipe (such as a DP meter) is termed a minor loss. However, it can still be significant. Again, any DP meter (or pipe component) is useable for the following example. Consider incompressible flow across a Venturi meter (see Figure 3). The energy equation for a horizontal meter applied between the inlet (point "1") and the point downstream where pressure recovery has been completed (point "3") can be written as equation 12:

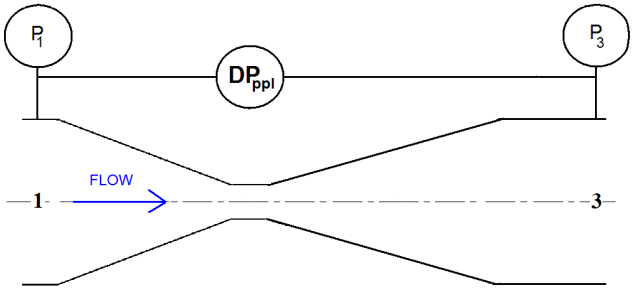

Fig 3. Generalised Permanent Pressure Loss Meter (Venturi sketch not to scale or dimensionally precise.)

$$\frac{P_1}{\rho}+\frac{U_1^{\,2}}{2}=\frac{P_3}{\rho}+\frac{U_3^{\,2}}{2}+h_{l\,m} \quad \text{---- (12)}$$

where P_1 and P_3 are the inlet and downstream pressures respectively, ρ is the fluid density, U_1 and U_3 are the inlet and downstream velocities respectively. DP meters are typically applied in pipe lines of constant[2] cross sectional area (A). Mass continuity shows the inlet and exit velocities are the same and therefore equation 12 reduces to equation 12a:

$$\dot{m}=\rho A_1 U_1=\rho A_3 U_3 \text{ ---- (1b)} \quad \text{and} \quad A_1=A_3 \text{ therefore } U_1=U_3$$

$$\frac{P_1-P_3}{\rho}=\frac{\Delta P_{PPL}}{\rho}=h_{lm} \quad \text{---- (12a)}$$

where $\Delta P_{PPL}=P_1-P_3$ is the PPL. It is fluid mechanics convention to express "minor head loss", i.e. the meters PPL, as multiples of the flows gas dynamic pressure:

$$\frac{\Delta P_{PPL}}{\rho}=h_{l\,m}=K_l\frac{U_1^2}{2} \quad \text{---- (12b)} \quad \text{and hence} \quad U_1=\sqrt{\frac{2\Delta P_{PPL}}{K_l\rho}} \quad \text{---- (12c)}$$

where K_l is termed the "minor loss coefficient". Substituting equation 12c into the equation 1b gives:

$$\dot{m}=A_1\sqrt{\frac{1}{K_l}}\sqrt{2\rho\left(P_1-P_3\right)}=A_1K_{PPL}\sqrt{2\rho\Delta P_{PPL}} \quad \text{---- (13)}$$

Note to simplify the equation a "permanent pressure loss coefficient", or "PPL coefficient", K_{PPL}, has been introduced as defined by equation 14:

$$K_{PPL}=\sqrt{\frac{1}{K_l}} \quad \text{---- (14)}$$

Most fluid mechanics text books list minor loss coefficients for various pipe components as constant values, i.e. suggesting minor loss coefficients are insensitive to Reynolds number. Munson et al [3] states:

"For many practical applications the Reynolds number is large enough so that the flow through the component is dominated by inertia effects, with viscous effects being of secondary importance…." and "In a flow that is dominated by inertia effects rather than viscous effects, it is usually found that pressure drops and head losses correlate directly with the dynamic pressure".

However, the traditional application of minor loss coefficients is to the prediction of approximate pressure losses through pipes. When creating a metering system, a lower level of uncertainty may be required. It may be necessary to account for a Reynolds number effect when calculating the PPL coefficient. (Note that

[2] DP meters with different inlet and exit cross sectional areas are called truncated meters. The methodologies described in this paper work with truncated meters after some modification of the equations.

when discussing minor pressure losses for orifice plate meters Miller [4] shows graphs of minor loss coefficients to Reynolds number for Re $\leq 10^4$ but for a general discussion on PPL he ignores any Reynolds number effect.) Furthermore, PPL's of gas flows cause the gas density to reduce. No expansion factor for such a metering system exists. A practical approach is to calibrate the PPL coefficient (which includes any expansion effect) against Reynolds number. It would then be an engineering judgment call on whether to use a constant value (allowing a direct solution to equation 13) or express the parameter as a function of the Reynolds number (and solve equation 13 by iteration of the mass flow rate).

2.e One DP Meter Body, Two DP transmitters, Three DP Flow Equations

DP meters typically have equal inlet and exit cross sectional areas. Therefore, as the fluid passes through the DP meters primary element (i.e. the obstruction) it flows first through a geometric constriction (expanding a gas flow) and then through a geometric expansion (compressing a gas flow) thus producing a permanent pressure loss. Hence, every DP meter has imbedded within it three metering opportunities: a conventional converging geometry meter (using the traditional differential pressure, ΔP_t), an expanding geometry meter (using the recovered DP, ΔP_r), and a PPL meter (using the permanent pressure loss, ΔP_{PPL}). A DP meter can be thought of as three flow meters in series in the same pipe location. For example, Figure 4 shows a sketch of a Venturi meter with DP transmitters to measure the three DP's of interest. Figure 4a shows a sketch of the approximate pressure fluctuations through a DP meter.

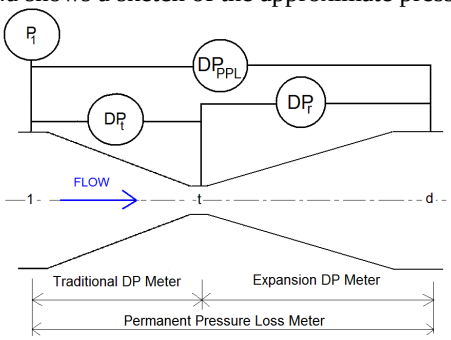

Fig 4. Venturi Meter with 3 DP measurements.

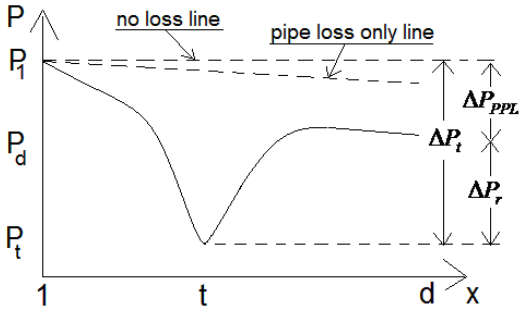

Fig 4a. Sketch of DP Meter Pressure Fluctuations.

Figure 4a shows a fundamental DP meter rule that the sum of the "recovered" DP (i.e. the downstream to minimum area or "throat" DP) and PPL is the upstream to throat DP. This can be expressed as equation 15 or equation 15a. (Note "PLR" is sometimes used to indicate the ratio of PPL to the upstream to throat DP.)

$$\Delta P_t = \Delta P_r + \Delta P_{PPL} \quad \text{--- (15)} \qquad , \qquad \frac{\Delta P_r}{\Delta P_t} + \frac{\Delta P_{PPL}}{\Delta P_t} = 1 \quad \text{--- (15a)}$$

Measuring any two of these DP's allows the calculation of the third DP and therefore only two DP transmitters are required to have all three equations available. Naturally, with ΔP_t being the largest value it is the easiest to measure accurately. The smaller values of ΔP_r and ΔP_{PPL} may have a higher measurement uncertainty. However, in the majority of applications all three DP's are of a magnitude where they can be measured to low uncertainty by standard DP transmitters. Measuring all three DP's produces the lowest uncertainty of DP measurement but measuring two DP's and deriving the third typically makes only a small increase to the third DP's uncertainty.

We can see from Figure 4's Venturi meter example that the traditional DP meter, geometric expansion DP meter and the PPL DP meter equations, which where each derived earlier in isolation, are all applicable to the same DP meter body. We see that $\beta = \beta'$ and $E = E'$, and switching the subscripts of 1, 2 & 3 to the DP meter body subscripts of "i" (for "inlet"), "t" (for "throat") and "d" (for "downstream") respectively, we can update equations 5a, 6a & 13 to equations 16, 17 & 18.

With the combination of three DP meter equations on one DP meter it is simplest to use the meter body inlet as the set gas density for all calculations. That is, the geometric expansion meter need not use its inlet density (i.e. the throat density). Hence, even though the density increases between the throat and the

$$\dot{m} = EA_t \varepsilon C_d \sqrt{2\rho(P_i - P_t)} = EA_t K \sqrt{2\rho\Delta P_t} \quad \text{--- (16)}$$

$$\dot{m} = E' A_t C_d' \varepsilon' \sqrt{2\rho(P_d - P_t)} = EA_t K_r \sqrt{2\rho\Delta P_r} \quad \text{--- (17)}$$

$$\dot{m} = A_i \sqrt{\frac{1}{K_l}} \sqrt{2\rho(P_i - P_d)} = A_i K_{PPL} \sqrt{2\rho\Delta P_{PPL}} \quad \text{---- (18)}$$

downstream pressure ports, at no time would the gas density be higher than the meter body inlet density and therefore in practice, even the geometric expansion meter equation could have an expansion factor.

Currently, with the expansion factors for any geometric expansion DP and PPL meters not being derived, these meters need to have flow coefficients that include the density variable effect. Note, that many DP meters need calibrated even for the traditional discharge coefficient or flow coefficient to be found, so all that is needed to calibrate a generic DP meter for all three equations (16 to 18) instead of the one traditional equation 16 is one extra DP transmitter. This means it is no more expensive and takes only marginally more effort to calibrate the extra two "meters" while calibrating the traditional meter.

2.f Relationships Between the Three Available DP Flow Meter Equations

To explain the principle of using the three flow equations together as a diagnostic tool the simplest case of incompressible flow with constant value flow coefficients is considered. (However, the methodology does work for compressible flow with flow coefficients varying with Reynolds number.) There is one generic DP meter body being considered. For from the law of conservation of mass we know that all three flow rate equations should (within their respective uncertainties) predict the same flow rate value. Therefore combining equation 16 to 18 gives equation set 19:

$$\dot{m} = EA_t K \sqrt{2\rho\Delta P_t} = EA_t K_r \sqrt{2\rho\Delta P_r} = A_i K_{PPL} \sqrt{2\rho\Delta P_{PPL}} \quad \text{--- (19)}$$

For a constant density and constant flow coefficients, all three equations (16 to 18) are parabolic equations. The mathematical equation for a parabola is $y^2 = 4ax$, where "a" is the parabolas focus. Squaring and equating equations 16 to 18 we get equation set 19a:

$$\dot{m}^2 = \{2\rho(EA_t K)^2\}\Delta P_t = \{2\rho(EA_t K_r)^2\}\Delta P_r = \{2\rho(A_i K_{PPL})^2\}\Delta P_{PPL} \quad \text{--- (19a)}$$

Now let: $a_t = \frac{\rho}{2}\{EA_t K\}^2$ --(20), $a_r = \frac{\rho}{2}\{EA_t K_r\}^2$ --(20a), $a_{PPL} = \frac{\rho}{2}\{A_i K_{PPL}\}^2$ --(20b)

i.e. a_t, a_r and a_{PPL} are the foci of three parabolic flow equations. Therefore we have equation set 19b:

$$\dot{m}^2 = 4a_t\Delta P_t = 4a_r\Delta P_r = 4a_{PPL}\Delta P_{PPL} \quad \text{--- (19b)}$$

Let us compare the relative magnitudes of these three foci. First, PPL is always present and positive, equation 15 therefore states that $\Delta P_t > \Delta P_r$ and therefore from equation set 19a we see that $EA_t K < EA_t K_r$ and hence from equations 20 and 20a we know that $a_t < a_r$. We also know that $\Delta P_t > \Delta P_{PPL}$ and therefore from equation set 19a we see that $EA_t K < A_i K_{PPL}$ and hence from equations 20 and 20b we can deduce that $a_t < a_{PPL}$. The relationship between a_r and a_{PPL} depends on the pressure recovery / PPL characteristics of a given DP meter. Different DP meter designs have significant differences in this respect. For example, the Venturi meter is a device that will recover the majority of the traditional differential pressure, the orifice plate meter is a device that will lose the majority of the traditional differential pressure where as some DP meter designs such as cone or nozzle meters will recover a moderate amount of the traditional differential pressure. Consider the case where the majority of the traditional differential pressure is recovered, i.e. $\Delta P_r > \Delta P_{PPL}$ (see Figure 5a). From equation set 19a we see for this condition that

$EA_tK_r < AK_{PPL}$. Hence we also know from equations 20a and 20b that for this condition $a_r < a_{PPL}$. Therefore, for the case of a DP meter where the majority of the traditional differential pressure is recovered the following meter characteristic is set:

$$a_t < a_r < a_{PPL}$$

Consider the case where the majority of the traditional differential pressure is lost, i.e. $\Delta P_r < \Delta P_{PPL}$ (see Figure 5b). Equation set 19a shows for this case that $EA_tK_r > AK_{PPL}$. Hence we also know from equations 20a and 20b that for this condition $a_r > a_{PPL}$. Therefore, for the case of a DP meter where the majority of the traditional differential pressure is lost the following meter characteristic is set:

$$a_t < a_{PPL} < a_r$$

Let us now consider the third and in reality rare case where the recovered DP and PPL are equal, i.e. $\Delta P_r = \Delta P_{PPL}$ (see Figure 5c). From equation set 19a we know $EA_tK_r = AK_{PPL}$. From equations 20a and 20b we know $a_r = a_{PPL}$. Therefore, for equal recovered and permanently lost DP's the following meter characteristic is set:

$$a_t < a_{PPL} \ , \ a_t < a_r \ , \ a_r = a_{PPL}$$

In this paper a three flow coefficient to Reynolds number plot is called a 3K plot and a flow rate to three DP plot (as seen in Figures 5a to 5c) is called a "PRT" plot (for "**P**ermanent Pressure Loss, **R**ecovered DP, **T**raditional DP mass flow rate plot").

The question remaining is do the two unconventional equations have acceptable uncertainty for practical use in real applications? Only if they do is there potential for the development of a diagnostic system. In section 3 the practicality of all three equations is demonstrated with multiple data sets. The data is shown in terms of 3K plots and PRT plots. Each meters data set can include different nominal pressures (i.e. gas densities) but as the flow coefficients are independent of gas density (other than through the second order effect of expansibility) the data in the 3K plots has been condensed such that the different pressures are not stated. Note that when a DP meter is traditionally calibrated the precise DP's, gas densities and Reynolds numbers at each point are recorded. However, as DP meter flow coefficients are independent of the fluid density it is not necessary to maintain a precise pressure and temperature across a turn down but rather just know what they are for each data point. This means most calibrations have only nominally set pressures and temperatures. As calibrations proceed there are typically slight pressure and temperature (and therefore gas density) shifts between points without this adversely affecting the calibration. However equations 20 to 20b show that the precise foci are dependent on density. Note that some of the following PRT plots are for chosen small density ranges and therefore *look* like they have moderate levels of scatter. Most of this is not scatter but the slightly varying density per point and it should be realized this is not therefore an indication of an uncertainty level of the three flow equations. The uncertainty levels (to 95% confidence) of the equations are only visible in the 3K plots.

Finally, note that if two of the three flow coefficients are known the third can be derived from the equations 15 to 18. The resulting relationship is shown as equation 21. However, even if the flow coefficient is known prior to calibration, in order to find either one of the expansion flow coefficient or the PPL coefficient, calibration is usually required. Therefore, as calibration is required to obtain a second flow coefficient and as it is as straight forward to calibrate all three flow coefficients at the same time as to calibrate one flow coefficient only, equation 21 is shown for academic completeness only. In reality the meters would be calibrated. Equation 21 can check calibration results to assure the results are reasonable.

$$K = \varepsilon C_d = \frac{K_r K_{PPL}}{\sqrt{K_{PPL}^2 + \left\{E^2 \beta^4 K_r^2\right\}}} \quad \text{--- (21)}$$

3. DP Meter Data Sets

3.a Standard Orifice Plate Meters

Four orifice meter gas flow data sets are presented. A CEESI wet gas meter Joint Industry Project (JIP) tested 4" orifice meters of beta ratios 0.3414, 0.4035, 0.4965 and 0.6826. All had the PPL measured using

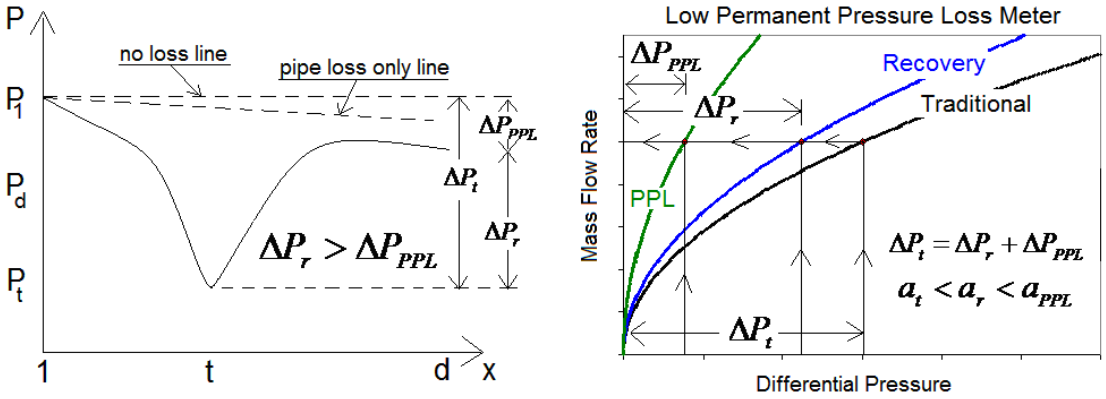

Fig 5a. Pressure fluctuation through DP meter where majority of DP is recovered (PLR < ½) and the associated three parabolic flow rate equations.

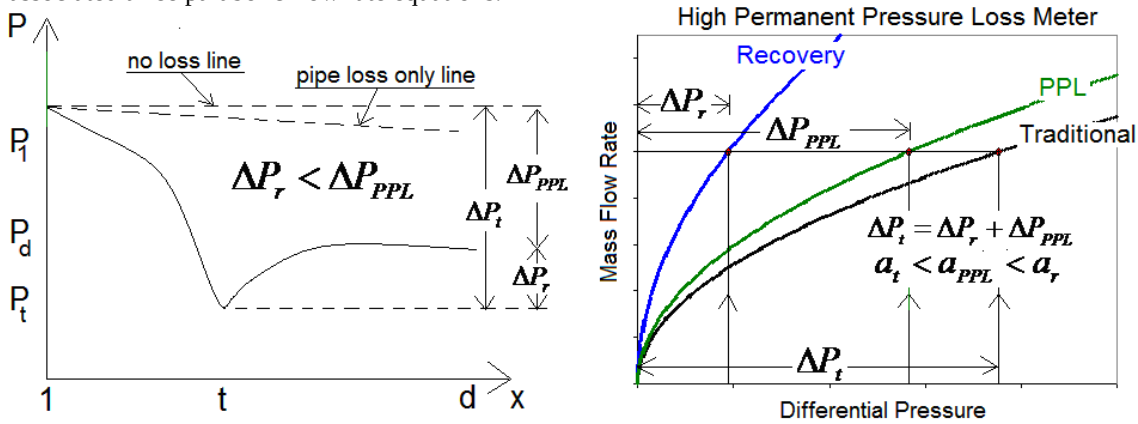

Fig 5b. Pressure fluctuation through DP meter where majority of DP is lost (PLR > ½) and the associated three parabolic flow rate equations.

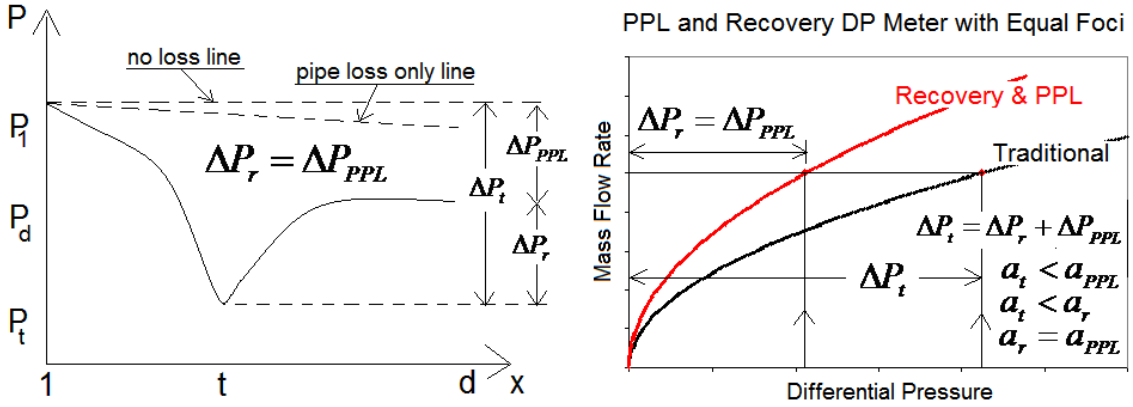

Fig 5c. Pressure fluctuation through DP meter where DP lost and recovered are equal (PLR = ½) and the associated three parabolic flow rate equations.

a downstream tapping located in accordance with ISO 5167 [5], i.e. 6 pipe diameters (6D) downstream of the plate. The PPL transmitter had an upper range limit (URL) of 400"WC (i.e. approximately 1 Bar) so data with DP's <10"WC were disregarded. The facility was a wet gas test facility (i.e. not a gas meter calibration facility) and the primary test purpose was to establish a gas flow baseline for wet gas flow tests. It was not a test to develop a DP meter diagnostic system. The mass flow reference meter was a turbine meter with an uncertainty of ±0.53% (Kegel [6]). The test set up is shown in Figure 6. Figures 7 to 10 show the CEESI JIP orifice meters 3K and PRT plots. The pressure ports were read from top dead centre.

All four orifice meters had discharge coefficients that were within the uncertainty limits of the Reader-Harris Gallagher (RHG) equation (ISO 5167 [5]). The orifice meter has a relatively high PPL. Figures 7

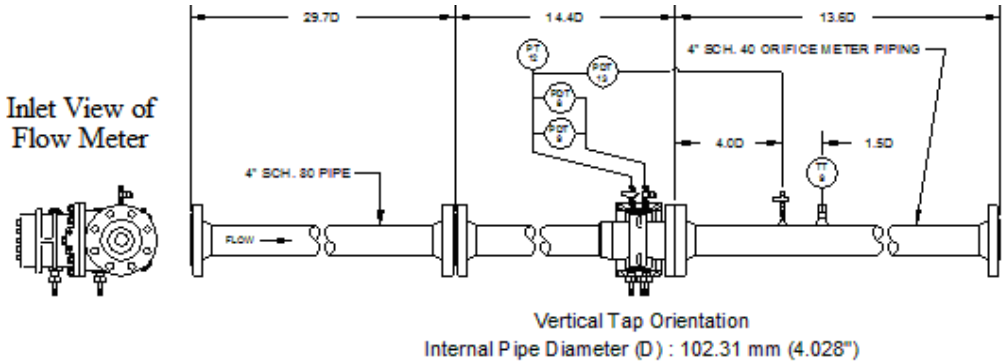

Fig 6. The CEESI JIP orifice meter set up.

to 10 show results as theoretically predicted and shown in Figure 5b. Also, as beta ratio increases there is a decrease in PPL and an increase in recovered pressure thus leading to an increase in the PPL coefficient and a reduction in the expansion flow coefficient values.

All four orifice meter results showed that across relatively large turn downs (up to 9:1), ignoring any gas expansion effects on equations 17 & 18, and using constant coefficient values instead of fits to the Reynolds number, after calibration, the traditional metering method had an uncertainty of < ±1%, while the non-standard methods had uncertainties < ±1.5%. These are meter uncertainty levels of practical use and therefore equations 17 & 18 are capable of being useful as part of a DP meters self diagnostic system.

Figures 7 to 10 show that the discharge coefficient is mildly sensitive to beta ratio where as the expansion flow and PPL coefficient are very sensitive to beta ratio. ISO 5167 [5] offers a method of estimating an orifice plate's minor loss coefficient (equation 22):

$$K_l = \left(\left(\frac{\sqrt{1-\left(\beta^4\left(1-C_d^2\right)\right)}}{C_d\beta^2} \right) - 1 \right)^2 \quad \text{--- (22)}$$

ISO therefore implies a method for predicting the orifice meter PPL coefficient without calibration as the RHG discharge coefficient prediction can be substituted into equation 22 to find the minor loss coefficient, meaning the PPL coefficient can be found by equation 14. ISO also approximates the orifice meter PLR as shown in equation 23. Furthermore, manipulation of equations 9, 19, 15 and 23 gives equation 24. The orifice meter expansion flow coefficient is therefore predictable via ISO.

$$PLR = \frac{\Delta P_{PPL}}{\Delta P_t} = 1-\beta^{1.9} \quad \text{--- (23)} \quad \text{therefore} \quad K_r = \frac{\varepsilon C_d}{\sqrt{1-\left(\frac{\Delta P_{PPL}}{\Delta P_t}\right)}} = \frac{K}{\sqrt{1-PLR}} = \frac{K}{\sqrt{\beta^{1.9}}} \quad \text{--- (24)}$$

It is therefore possible to compare ISO information derived predictions with calibrated values. In practice a gas flow has expansibility and the discharge coefficient varies slightly with the Reynolds number. It is therefore simpler here, as a first look, to approximate the orifice meter discharge coefficient to a set value of 0.6 when predicting the PPL and expansion flow coefficients. Table 1 shows these results for the four CEESI JIP orifice meters tested. The ISO equations for orifice meter PLR's and minor loss coefficients are designed to give approximate estimates of the PPL the meter will induce on the flow. They are not stated to be precise predictions. Table 1 shows that most ISO derived predictions are close to the test results.

Meter (beta)	Test Kr	"ISO" Kr	%diff Kr	Test Kppl	"ISO" Kppl	%diff Kppl	Test PLR	ISO PLR	%diff PLR
0.3414	1.6220	1.6655	2.68	0.0748	0.0755	0.996	0.8663	0.8702	0.45
0.4035	1.3990	1.4210	1.57	0.1088	0.1093	0.455	0.8155	0.8217	0.76
0.4965	1.1690	1.1669	-0.18	0.1790	0.1777	-0.734	0.7327	0.7356	0.39
0.6826	0.9000	0.8624	-4.18	0.4360	0.4312	-1.104	0.5444	0.5159	-5.23

Table 1. Comparisons of test results to ISO 5167 predictions.

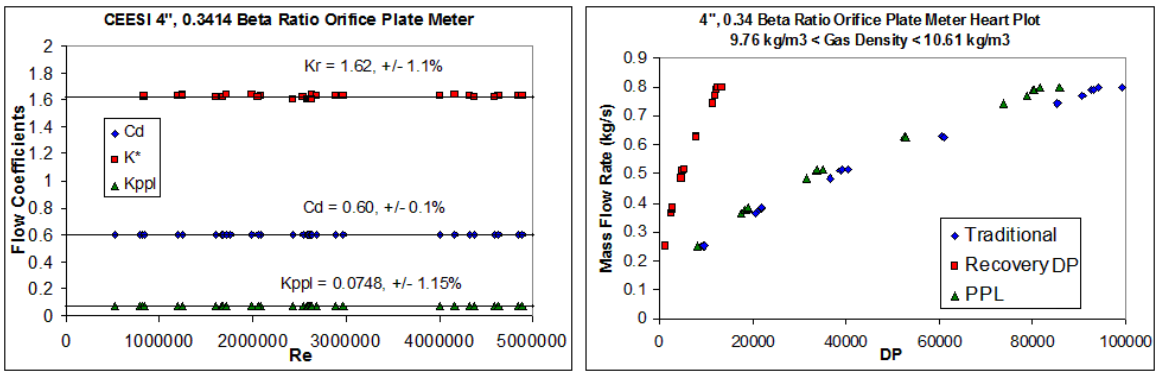

Fig 7. CEESI Wet Gas JIP 4", 0.3414 Beta Ratio Orifice Plate Meter Dry Gas Data.

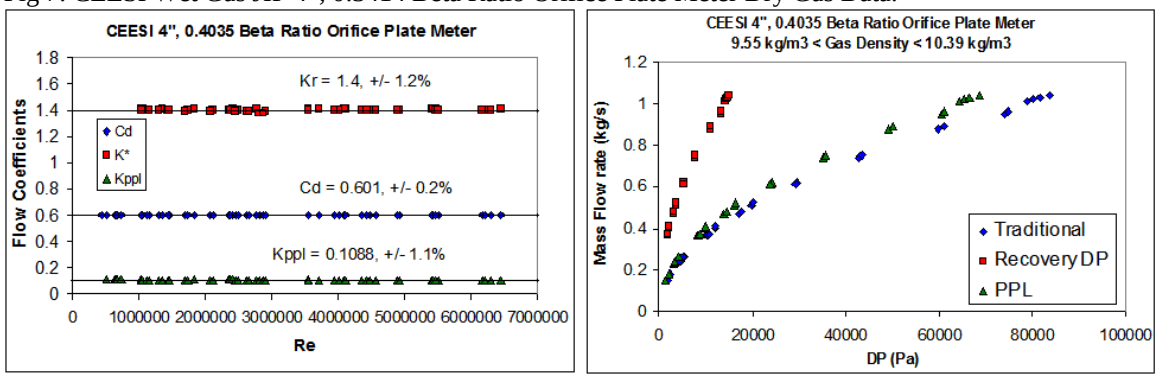

Fig 8. CEESI Wet Gas JIP 4", 0.4035 Beta Ratio Orifice Plate Meter Dry Gas Data.

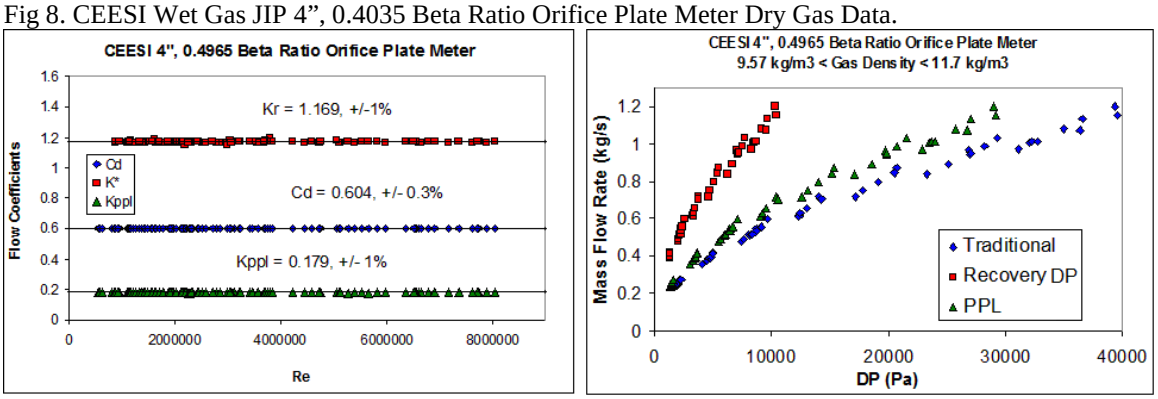

Fig 9. CEESI Wet Gas JIP 4", 0.4965 Beta Ratio Orifice Plate Meter Dry Gas Data.

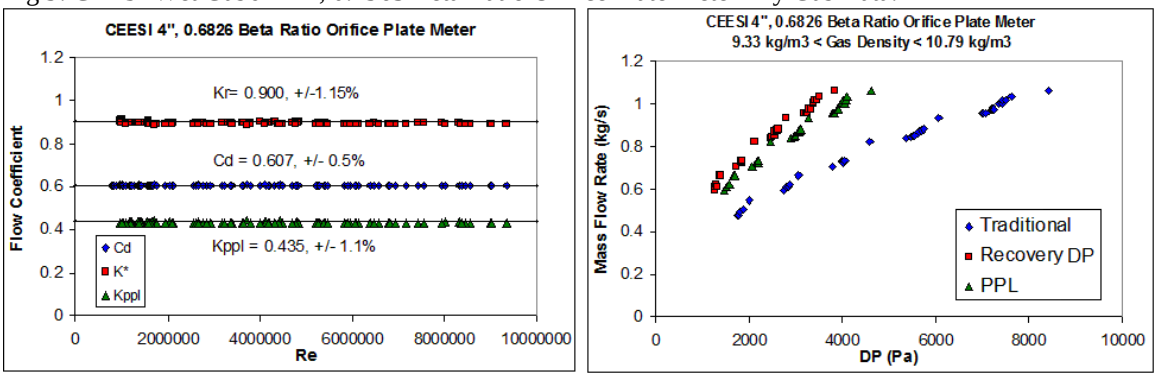

Fig 10. CEESI Wet Gas JIP 4", 0.6826 Beta Ratio Orifice Plate Meter Dry Gas Data.

However, there are cases where the differences are > 4%. Therefore, for equations 17 & 18 to be practically useful orifice meter expansion flow and PPL coefficients should be found by calibration.

3.b Standard Venturi Meters

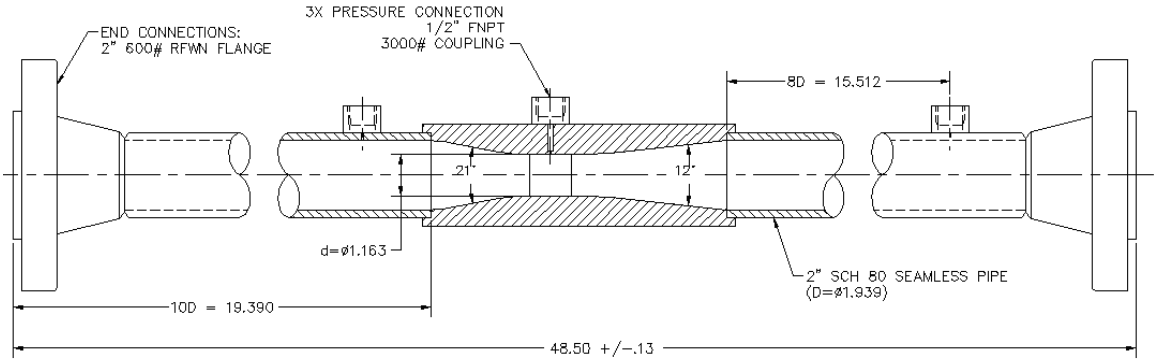

Fig 11. 2", 0.6 Beta Ratio Venturi Meter

CEESI commissioned a 2" wet gas multiphase flow facility in 2004 and gas flow data from a 2", 0.6001 beta ratio, 12^0 diffuser angle Venturi was recorded (see Figure 11). The PPL was measured via a pressure tap located on the meter body at 8D from the diffuser exit (i.e. a longer distance than recommended by ISO [5]). CEESI upgrades to the 4" wet gas test facility in 2007 included a commissioning gas run with a 4", 0.6001 beta ratio, 15^0 diffuser angle Venturi meter installed. The PPL was measured via a pressure tap located in a downstream spool 6D from the diffuser exit (i.e. in accordance with ISO [5]). In both cases the PPL transmitters had an URL of 400"WC. Due to the Venturi meter having relatively low PLR's, most of the PPL's read were < 10"WC and therefore data was accepted at DP <5"WC at the cost of increased uncertainty. Both test systems reference meters had uncertainties of < ±1%. Pressures were read from top dead centre of the meters. Figure 12 & 13 shows the 3K and PRT plots.

ISO [5] states that "Research into the use of Venturi tubes in high-pressure gas [≥ 1 MPa (≥ 10 bar)] is being carried out at present…" and "In many cases for Venturi tubes with machined convergent sections discharge coefficients which lie outside the range predicted by this part of ISO 5167 by 2% or more have been found. For optimum accuracy Venturi tubes for use in gas should be calibrated over the required flowrate range." Furthermore, the discharge coefficients stated in the standard for machined convergent sections are only valid for Reynolds numbers less than one million. That is, if the pressure is higher than 10 bar and / or the Reynolds number is greater than one million calibration is suggested. There are also independent verifications of Venturi meters giving unpredictable discharge coefficients (e.g. Geach et al [7]). Therefore, if a Venturi is being calibrated to find the traditional discharge coefficient there is little more effort to add an extra DP transmitter and calibrate all three equations 16 to 18.

ISO [5] does not offer PLR predictions for Venturi meters but Miller [4] states that the PLR of a Venturi with a 15^0 diffuser angle can be predicted by equation 25. (This is an approximate equation.) Using Millers equation 25, a PLR prediction can be found and from this an expansion flow coefficient can be predicted by considering equations 9, 15a, 19 & 25. This prediction is shown as equation 26. The PPL coefficient can be predicted by considering equations 3, 9, 14 & 19. The PPL coefficient is therefore given by equation 27. Figures 12 & 13 shows results as theoretically predicted (see Figure 5a). Table 2 shows the results of comparing the Miller PLR prediction based values and the test results.

$$PLR = \frac{\Delta P_{PPL}}{\Delta P_t} = 0.436 - (0.86\beta) + (0.59\beta^2) \quad \text{--- (25)}$$

$$K_r = \frac{\varepsilon C_d}{\sqrt{1 - \left(\frac{\Delta P_{PPL}}{\Delta P_t}\right)}} = \frac{K}{\sqrt{1 - PLR}} \quad \text{--- (26)}$$

$$K_{PPL} = \frac{1}{\sqrt{K_l}} = \left\{\frac{E\beta^2}{\sqrt{PLR}}\right\} K = \left\{\frac{E\beta^2}{\sqrt{PLR}}\right\} \varepsilon C_d \quad \text{--- (27)}$$

The 4" Venturi's discharge coefficient showed some variation with Reynolds number and a tendency for discharge coefficients to be larger than unity (as shown by Geach et al [7]). The discharge coefficient of 1.003 is considered a reasonable result. The 4" Venturi data and all the coefficient predictions are shown to

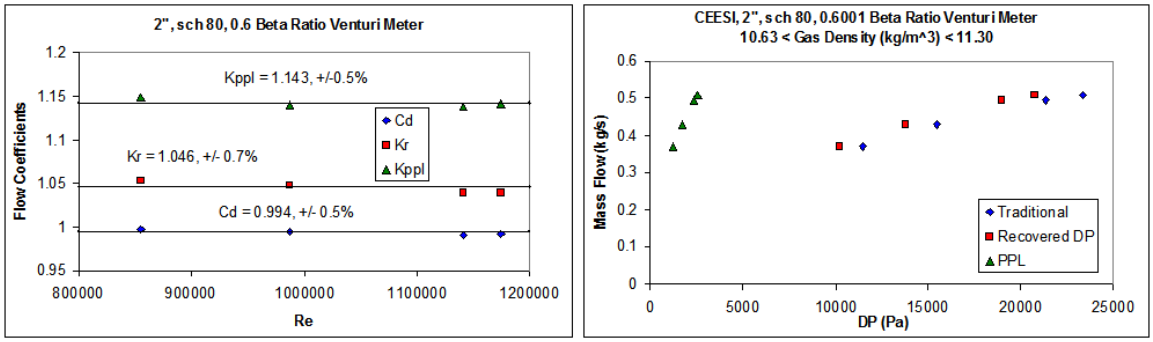

Fig 12. CEESI Wet Gas Flow Facilities Commissioning 2", 0.60 Beta Ratio Venturi Meter Dry Gas Data.

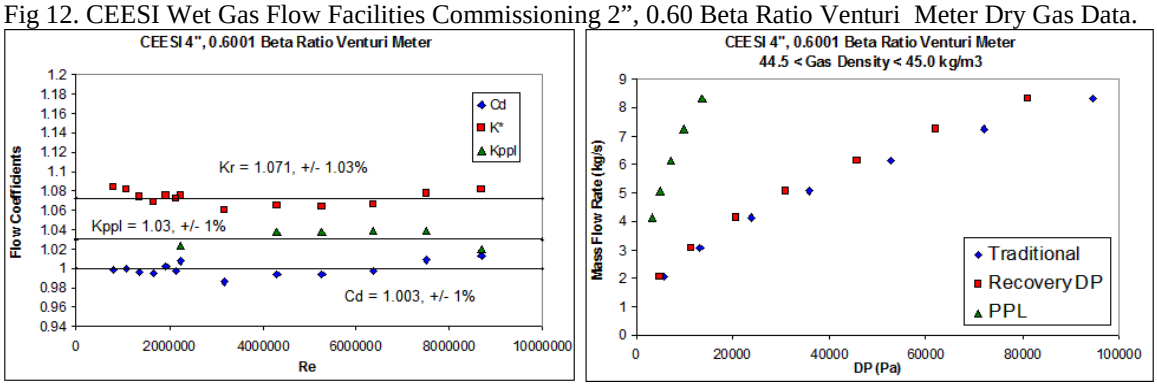

Fig 13. CEESI Wet Gas Flow Facilities Commissioning 4", 0.60 Beta Ratio Venturi Meter Dry Gas Data.

Meter size	Test Kr	"Miller" Kr	% diff Kr	Test Kppl	"Miller" Kppl	%diff Kppl	Test PLR	Miller PLR	%diff PLR
2"	1.046	1.078	3.1	1.143	1.060	-7.3	0.111	0.1324	19.3
4"	1.071	1.078	0.7	1.030	1.060	2.9	0.140	0.1395	-0.4

Table 2. Comparisons of test results to Miller PLR prediction derived predictions.

be in reasonable agreement. *After calibration* the three 4" Venturi flow coefficients all gave flow rate predictions to ≤ ±1.03%. The available 2" Venturi data has a very small Reynolds number range (a turn down of 1.37:1) so little can be said regarding the flow coefficient's relationships with Reynolds number. All three 2" Venturi flow coefficients were fitted to constant values and *after calibration* they each gave flow rate predictions to ≤ ±1%. However, the 2" data had a larger discrepancy than the 4" data with the Miller PLR prediction based values (see Table 2). These differences are not judged extreme, and as the Miller PLR prediction is an approximation (and for a slightly different diffuser angle) this is not a significant issue. However, calibration is required to accurately predict the Venturi meter flow coefficients. Both Venturi meter result showed that, by ignoring gas expansion effects on equations 17 & 18, and using constant coefficient values instead of fits to the Reynolds number, *after calibration*, all three flow predictions (equations 16 to 18) gave uncertainty levels of practical industrial use. Therefore these metering methodologies are capable of being useful as part of a Venturi meters self diagnostic system.

3.c Cone DP Meters

Three cone meter data sets are presented. The cone meter is not listed in the standards and no PLR prediction is offered by Miller. Hence no flow coefficient predictions are made here. BG Group tested a 6", 0.75 beta ratio V-Cone meter with natural gas flow at K-Lab with the PPL measured via a tapping 6D from the back face of the cone. The data has been released to this author. The URL of the traditional DP and PPL transmitters at K-Lab are unknown. The readings were as high as 522"WC (i.e. approximately 1.3 bar) so any DP's <10"WC were removed as potentially high uncertainty points.

CEESI has a 4", 0.7499 beta ratio generic cone meter installed permanently in the wet gas flow test facility. Figure 14 shows a sketch of this cone meter. This meter has the PPL measured via a pressure tapping located on the meter body at 3D downstream of the back face of the cone. (Note that there is no cone meter pressure recovery length stated in the literature. The choice of 3D as a suitable location for the downstream pressure tap was therefore engineering judgment only.) This meter was initially gas calibrated in a CEESI

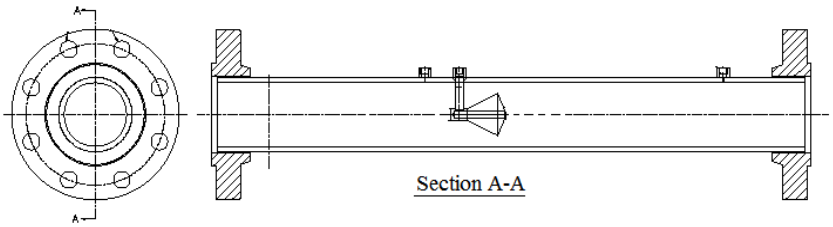

Fig 14. A Sketch of a Generic Cone DP Meter.

gas blow down facility. All DP's read were within range of the DP transmitter ranges used. The traditional DP and PPL's were recorded. The reference gas meter had an uncertainty was ±0.5%.

The third data set is from a different 4", 0.75 beta ratio generic cone meter tested at a CEESI air flow facility. The PPL was measured via a pressure tapping located in a downstream spool again at 3D from the back face of the cone. The PPL transmitter had an URL of 400"WC and therefore any DP's <10"WC were disregarded. The reference flow meter was a critical nozzle with an uncertainty of ±0.5%.

Figures 15 to 17 show the three cone meter 3K and PRT plots. The discharge coefficients of the three cone meters are all[3] in the vicinity of 0.8. However, the spread of $0.787 < C_d < 0.809$ is typical of cone meters. Furthermore, even though the three meters are similar designs (although the K-Lab meter is 6" with a different downstream pressure tap location) the expansion flow coefficient and the PPL coefficient values vary between each meter. Note that in Figure 15, PLR ≈ ½ as $a_r \approx a_{PPL}$. However Figure 16 has $a_t < a_{PPL} < a_r$ (i.e. PLR >½) and Figure 17 has $a_t < a_r < a_{PPL}$ (i.e. PLR <½). These differences are likely due to manufacturing inconsistencies. (It is generally thought more expensive and time consuming to produce identical cone meters than identical orifice meters.) It is not yet possible to accurately predict any of the cone meter flow coefficients so calibration is required. Nevertheless, it has previously been shown calibration of the expansion flow coefficient and the PPL coefficient would also be required for the orifice and Venturi meters. (In fact, ISO [5] state for certain flow conditions, calibration of the Venturi meter discharge coefficient may also be required.) *After calibration*, ignoring expansion effects and using constant values only instead of Reynolds number fits, all three cone meters had all three flow equations (16 to 18) predicting flow rates to an uncertainty ≤ ±1%. This again offers proof that any DP meter can be calibrated to give all three flow equations to an industrially useful uncertainty level. (It is assumed here that the expansion and PPL flow coefficients will be found to be as repeatable as discharge coefficients.)

Note that the cone meter will behave in the same way as other DP meters. Increasing the beta ratio (i.e. reducing the cone size) reduces the PLR thereby reducing the expansion flow coefficient and increasing the PPL coefficient. Finally note that the cone meter is marketed as having a discharge coefficient largely immune to upstream flow disturbances (see Peters et al [8]). It is not currently known what effect upstream flow disturbances would have on cone (or any DP) meters expansion and PPL flow coefficients.

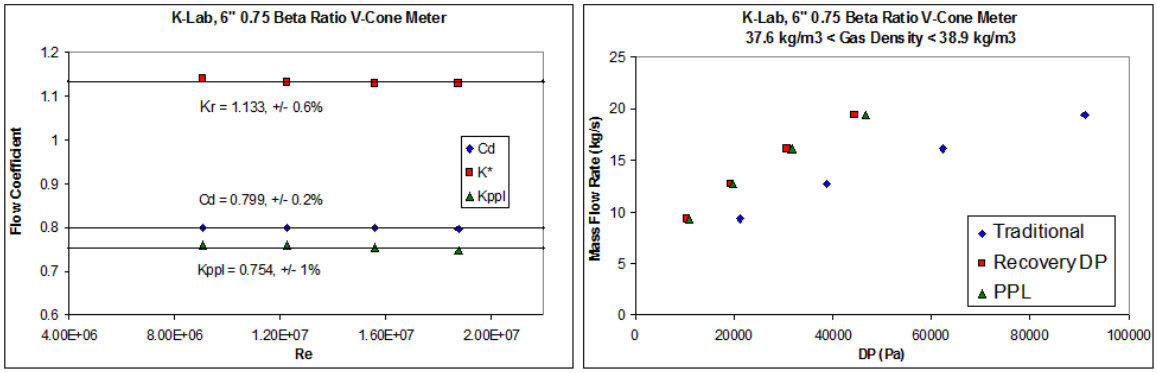

Fig 15. K-Lab Wet Gas Flow Facilities 6", 0.75 Beta Ratio V-Cone Meter Dry Gas Data.

[3] This CEESI air flow data had several gas velocities in excess of the typical industry maximum of 30 m/s. These data points, especially at lower pressures, had significant expansibility effects. They were removed from the data presented here to be discussed in proper context in Section 5.

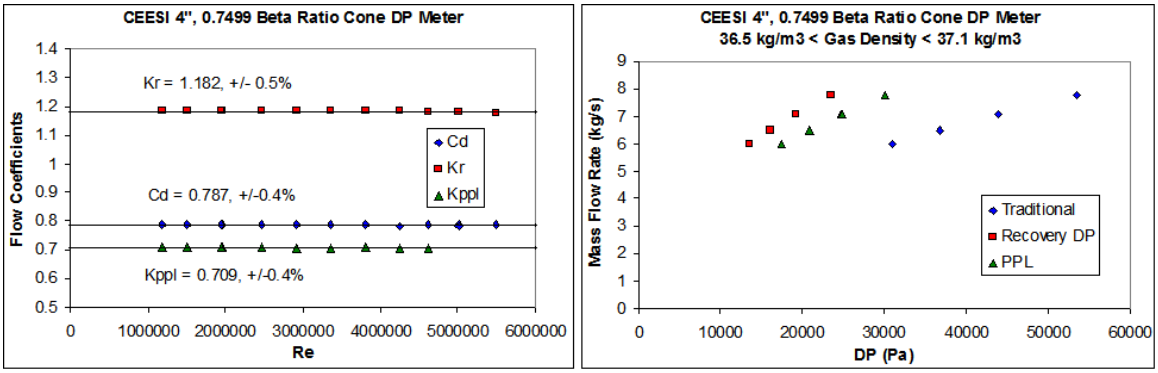

Fig 16. CEESI Air Blow Down Calibration, 4", 0.7499 Beta Ratio Cone DP Meter Dry Gas Data.

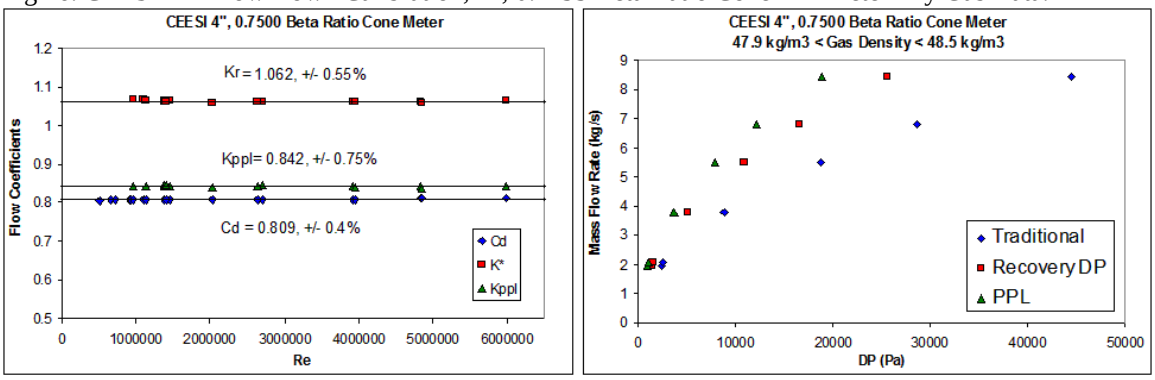

Fig 17. CEESI Air Blow Down 4", 0.7500 Beta Ratio Cone DP Meter Dry Gas Data.

3d. <u>A 4", 0.791 Beta Ratio Wedge Meter & a 4", 0.5 Beta Ratio Eccentric Orifice Plate Meter</u>

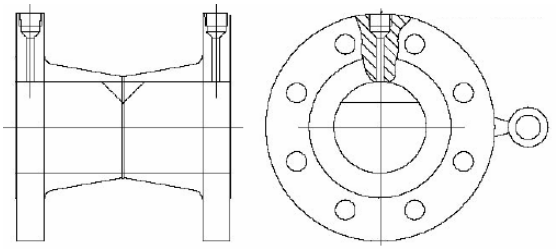

Fig 18. Wedge Meter

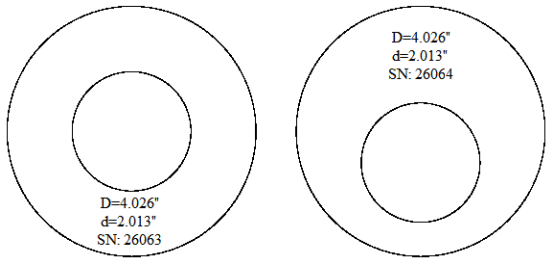

Fig 19. Standard & Eccentric Orifice Plate Designs.

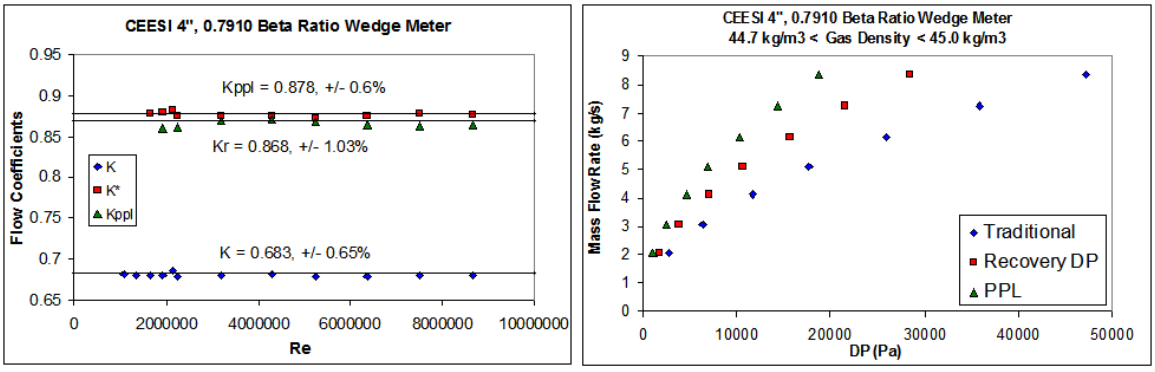

Fig 20. CEESI Wet Gas Facilities Commissioning 4", 0.7910 Beta Ratio Wedge DP Meter Dry Gas Data.

CEESI tested a 4", 0.791 beta ratio wedge meter (see Figure 18) and a 4", 0.500 beta ratio eccentric orifice plate meter (Figure 19) with dry natural gas flows. The wedge was located top dead centre and the orifice located bottom dead centre. There are no standards available for wedge or eccentric orifice meters and therefore neither meter has stated downstream length requirements to assure maximum pressure recovery.

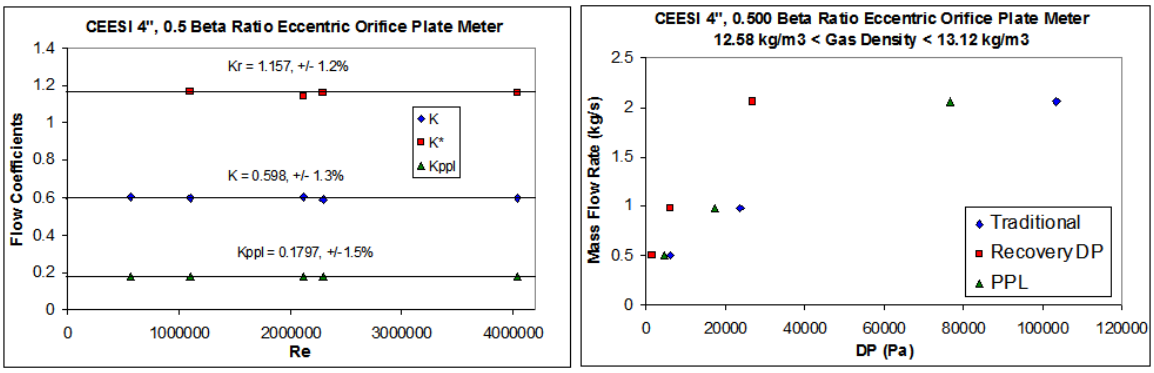

Fig 21. CEESI Wet Gas Facilities 4", 0.500 Beta Ratio Eccentric Orifice Plate Meter Dry Gas Data.

The PPL's were read via ports on downstream spools at 6D from the low pressure ports. PPL transmitters with URL's of 400"WC were used and data with DP's < 5"WC were disregarded. The reference meter had an uncertainty of ±0.53%. The pressure taps where at top dead centre.

Figures 20 and 21 show the wedge and eccentric orifice meter 3K and PRT plots respectively. As there are no expansion factors available for these DP meters the traditional calibrations use the flow coefficient, K. The wedge meter flow coefficient had a < ±0.7% uncertainty and the expansion and PPL flow coefficients had uncertainties ≤ ±1.03%. The average PLR of the wedge meter was 0.395 and hence the majority of the traditional DP is recovered. The PRT plot shows that the wedge meter data behaves as predicted in section 2f (i.e. it matches Figure 5a). The eccentric orifice meter flow coefficient had a < ±1.3% uncertainty and the expansion and PPL flow coefficients had uncertainties < ±1.5%. The average PLR of the eccentric orifice meter was 0.73 and hence the majority of the traditional DP is lost. The PRT plot shows that the eccentric orifice meter data behaves as predicted in section 2f (i.e. it matches Figure 5b). Hence, for both the wedge and eccentric orifice meters, equations 16 to 18 could be of practical industrial use.

3f. 4", Vortex Meter with an Effective 0.78 Beta Ratio

CEESI tested a VorTek Instruments 4" vortex meter with air flow. The vortex meter is not a DP meter by design. However, the fluid mechniacs phenomena being discussed here is applicable to any DP meter primary element, or any pipe obstruction, even those not principally designed as primary elements for DP meters. The VorTek Instrument vortex meter was ideal for this research as the meter body had pressure taps both upstream and adjacent to the vortex shedding bluff body[4]. A sketch is shown in Figure 22.

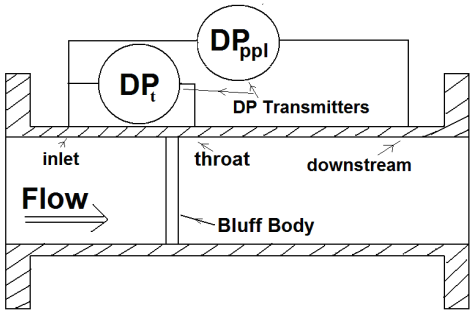

Fig 22. Sketch of the Vortex Meter with Two DP Transmitters Installed.

The effective beta ratio was 0.78 (when treating the bluff body as a DP meters primary element). The PPL was read via a downstream tap on the meter spool 3D from the bluff body. The PPL transmitter had a URL of 400"WC so data with DP's < 10"WC were disregarded. The reference meter was a critical nozzle with ±0.5% uncertainty. This test had an extremely large turndown and several points had velocities well in excess of 30 m/s. This data has been removed here as it is of limited practical industrial use and had a significant expansion effect. This effect is discussed more in Section 5.

[4] This vortex meter design has a pressure tap at the bluff body to allow the local pressure to be measured at the point of vortex shedding. This is claimed by the manufacturer to allow a more precise density prediction at the point of vortex shedding, thereby making a more accurate gas mass flow rate meter.

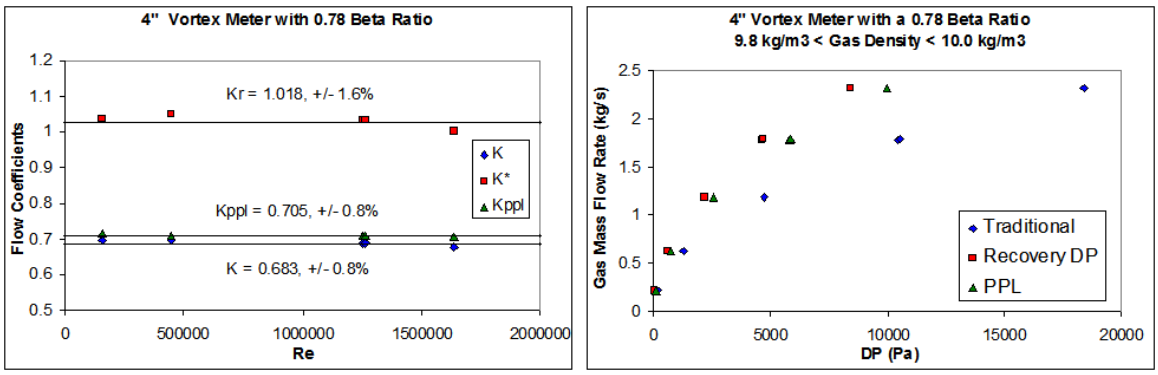

Fig 23. Low and Moderate Velocity CEESI Test Data on Vortex Meter Set Up as a DP Meter.

The effective beta ratio was 0.78 (when treating the bluff body as a DP meters primary element). The PPL was read via a downstream tap on the meter spool 3D from the bluff body. The PPL transmitter had a URL of 400"WC so data with DP's < 10"WC were disregarded. The reference meter was a critical nozzle with ±0.3% uncertainty. This test had an extremely large turndown and several points had velocities well in excess of 30 m/s. This data has been removed here as it is of limited practical industrial use and had a significant expansion effect. This effect is discussed more in Section 5.

Figure 23 shows the vortex meter 3K and PRT plots. With no expansion factor available the flow coefficient is used. This had a 0.8% uncertainty. The expansion and PPL flow coefficients had uncertainties < ±1.6%. Hence, equations 16 to 18 apply to the vortex meter and these equations could be integral to a practical vortex meter diagnostic tool. The average PLR was approximately 0.55 (i.e. PLR > ½). Note that the PRT plot (see Figure 23) agrees with the theory described in Section 2f for this case (see Figure 5b).

4. <u>DP Meter Data with Short Downstream Pressure Tapping Distances</u>

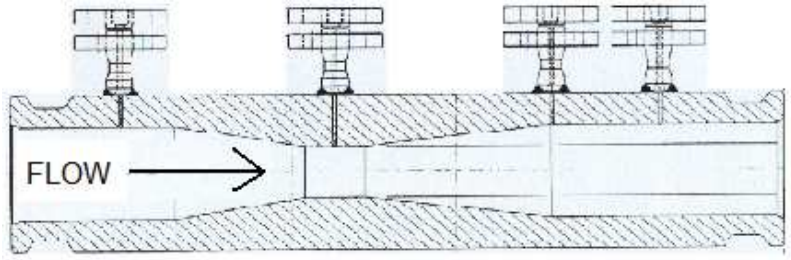

Fig 24. ISA Controls, 6", 0.55 Beta Venturi Meter Tested at NEL.

One issue with applying the concept of the downstream pressure tap to DP meters is overall meter length. ISO [5] states orifice and Venturi meters should be given 6D to recover all the recoverable pressure. For moderately large meters this can become a relatively long distance. It is of interest to see the effect of shortening this distance to place the downstream tap in a location where the flow may still be decelerating / compressing. There are two available data sets that allow this investigation. Neither meter was tested in this way deliberately.

In 1998 ISA Controls built a 6", 0.55 beta ratio standard Venturi for this authors PhD wet gas testing at NEL (see Figure 24). Note the two downstream taps. One is at the junction of the diffuser exit and the other is 1D further downstream. These downstream taps are far short of ISO's suggested 6D location. This Venturi was tested in dry and wet gas flows with the 1D downstream tap used. The dry gas results are shown in Figure 25. The discharge coefficient had an uncertainty of 0.7% while the expansion flow coefficient had an uncertainty of 1.3%. These values are in line with the other DP meter data sets. However, the PPL coefficient had a relatively large uncertainty of 5%.

The traditional DP and the PPL were measured directly. The recovery DP was derived by equation 15. The PPL was considered an add on to the main test purpose so the last available transmitter was used. This had a URL of 750"WC. The result was the gas PPL data were all at <8% of the transmitters range (and PPL's > 10"WC were accepted). It was for this project in 1998 that the author first derived equations 17 & 18. The

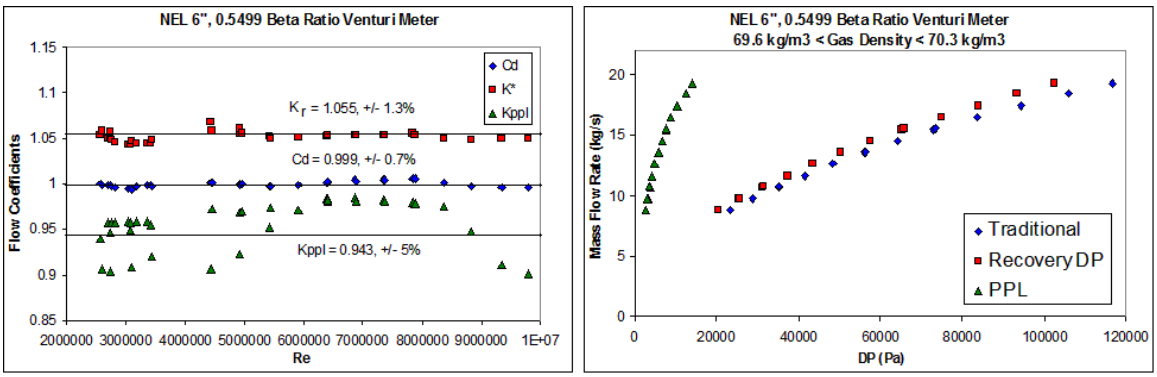

Fig 25. ISA Controls 6", sch 80, 0.55 Beta Ratio Venturi Meter with Short Downstream Pressure Tapping.

"PPL" metering method was dropped due to this poor result. However, it is noteworthy that the PLR was 0.112 (±9%), i.e. close to the expected full pressure recovery of a Venturi (e.g. see Table 2). Therefore, the majority of the pressure recovery had taken place by 1D downstream of the diffuser. The scatter is therefore considered largely due to the significant uncertainty in the PPL values. The expansion flow meter concept worked reasonably because the absolute values of the PPL's were relatively small, so even relatively large percentage errors in PPL measurement did not cause relatively large percentage errors in recovery DP estimation by equation 15. Figure 25 agrees with the theory of Section 2f (and Figure 5a).

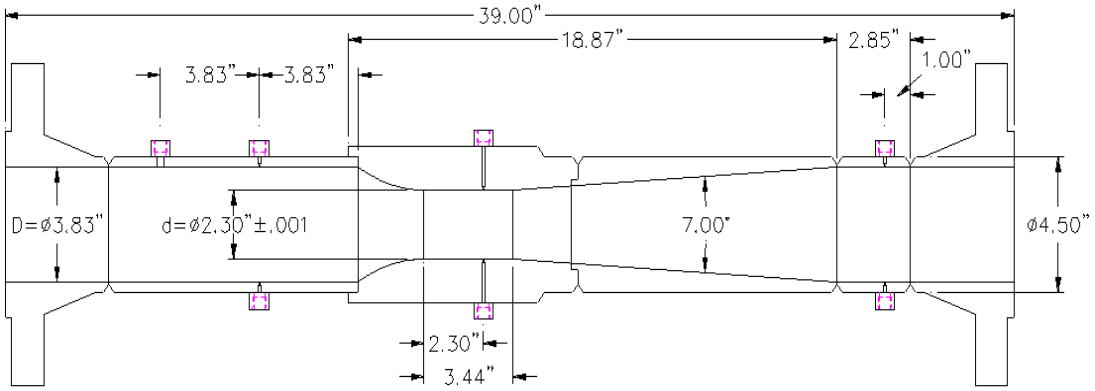

Fig 26. CEESI 4", 0.6 Beta Ratio Circular Arc Inlet Venturi Meter.

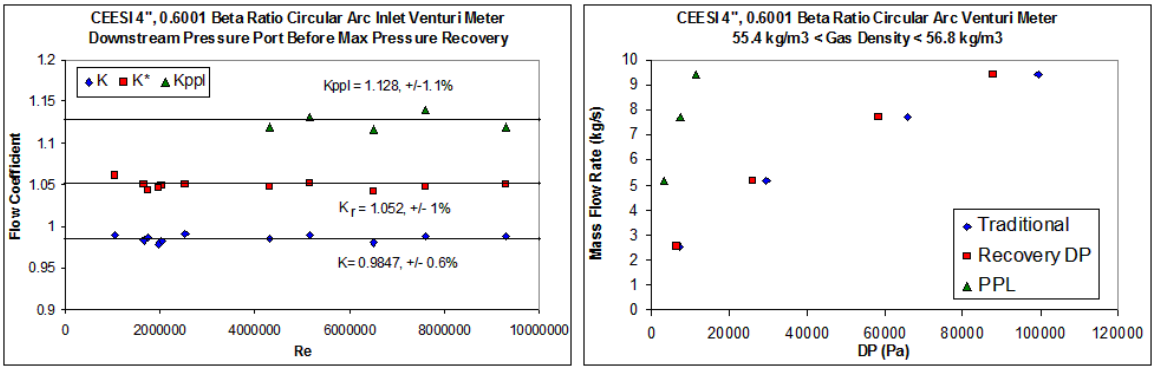

Fig 27. JIP 4", 0.6 Beta Ratio Circular Arc Venturi Meter.

The CEESI wet gas JIP natural gas flow tested a 4", 0.60 beta ratio circular arc inlet Venturi meter with a downstream tap in the meter body ½ D downstream of the diffuser exit (see Figure 26). Figure 27 shows the resulting 3K and PRT plots. The reference meter had an uncertainty of ±0.53%. The PPL transmitter had a URL of 125"WC and all DP's < 10"WC were discarded. The low PPL values were therefore more accurately measured in this case than for the classical Venturi meter case above. The flow coefficient, K, had uncertainties <±0.6% and expansion flow and PPL coefficients had uncertainties <±1.1%. The PLR was 0.118 (±6%). Therefore, again it appears the pressure recovery was largely complete just after the

diffuser exit. It is therefore debatable whether the expansion and PPL flow coefficients would be substantially different if the downstream tap was located much further downstream. Note that Figure 27 shows that this meter behaves as theory predicts (i.e. it matches Figure 5a).

More testing with different DP meter designs is required to make any definite comments regarding the effect of shortening the downstream pressure tap distance. The two examples here both appear to have fully (or close to fully) recovered pressures so there is limited information that can be taken from these data sets. However, from this limited evidence it appears that (as long as the DP's are read to a suitable uncertainty level) it is possible to calibrate these three flow coefficients to Venturi meters with shorter downstream tap locations than 6D. It is however probably good practice to have the downstream pressure tapping at the ISO suggested point of full pressure recovery if space allows.

5 Expansion Factor Issues

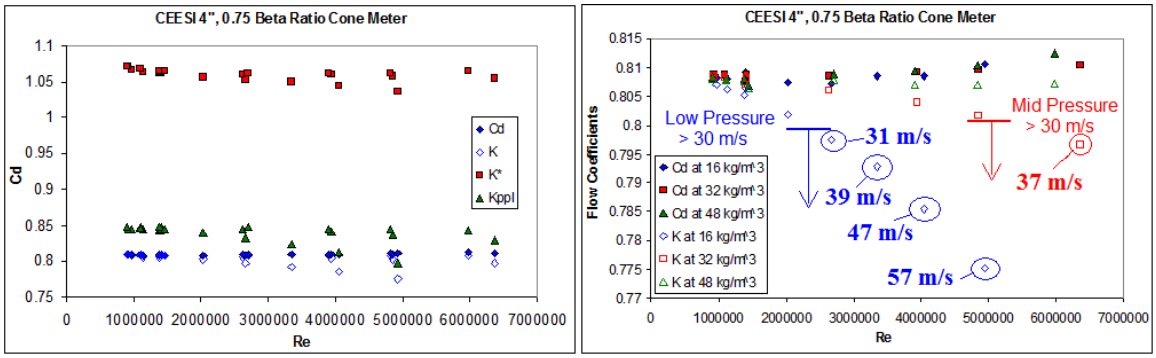

Fig 28. All CEESI Air Blow Down 4", 0.75 Beta Ratio Cone DP Meter Dry Gas Data.

In reality all three flow rate equations (16 to 18) will, for gas flows, be affected by density variations. Some DP meters have expansion factors (i.e. density corrections) for the traditional equation 16 but others do not. If an expansion factor (ε) exists the traditional meter is calibrated to the discharge coefficient (C_d). If no expansion factor exists a traditional meter is calibrated to the flow coefficient, K. However, for equations 17 & 18 there are, as yet, no expansion factors available for any meter.

If there is a high velocity gas flow through a meter with no expansion factor, any flow equation (16 to 18) will show a gas density effect. The higher the gas velocity, the lower the beta ratio and the lower the pressure, the larger this effect will be. Figure 28 shows an extreme example. The 4", 0.75 beta ratio cone meter had data with gas velocities > 30 m/s. Figure 17 is the data set shown in Figure 28 with the exception that the high velocity data (> 30 m/s) was removed. Here we see that adding the high velocity data significantly increases the spread of data. This is the gas density effect. Note that for the case of the discharge coefficient, C_d (which is independent of the expansion effect), there is no significant scatter. For the other three flow coefficients that are not isolated from the expansion effect, i.e. the flow coefficient (K), the expansion flow coefficient (K_r) and the PPL coefficient (K_{PPL}), the addition of the high gas velocity data has a distinct effect in increasing the data spread.

The right hand side plot in Figure 28 specifically shows the discharge coefficient, C_d, and the flow coefficient, K, at different gas densities, together as an example. The discharge coefficient is relatively constant (regardless of the test pressure and flow velocity). The flow coefficient is not constant and directly effected by the gas velocity and pressure. Above 30 m/s the effect becomes more significant. The most extreme divergence between discharge and flow coefficients is at the lowest density and highest velocity. This example is shown to indicate that the same issues are important to the expansion and PPL flow coefficients as are important to the flow coefficient. That is, when applying equations 17 & 18 you must take into account the same considerations you would when applying a flow coefficient instead of a discharge coefficient in equation 16. However, over a wide range of industrially practical gas flow rates the density variation effects are relatively small. Therefore, constant or Reynolds number fitted flow coefficients, expansion flow coefficients and PPL coefficients are industrially practical.

6 A Generic DP Meter Diagnostic System

With three flow equations for every DP meter (with two DP transmitters) there is redundancy in the

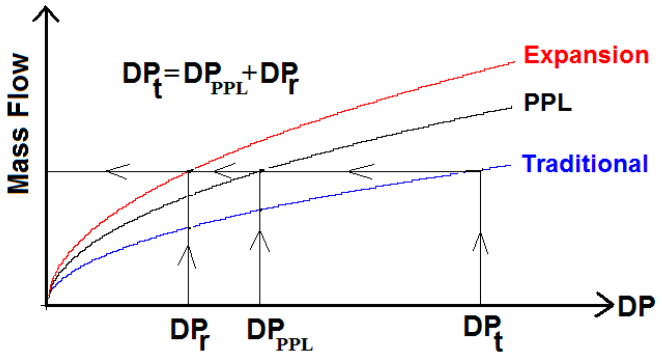

Fig 29. Sketch (not to scale) showing typical DP's and flow equations relationships.

metering system and an opportunity to develop diagnostic capabilities. Figure 29 indicates a typical relationship between the three DP's and the parabolic flow equations when a DP meter system (chosen randomly to have PLR > ½) is operating correctly. The PLR is constant for single phase flow through any DP meter. Therefore, if the meter is operating correctly all three flow equations must equal each other (within the normal uncertainties of the three metering techniques). Let us now discuss two possible DP meter problems:

1) Incorrect pressure or DP reading. (This can be caused by various issues such as blockage of a pressure port, impulse line leaks, open valves on DP transmitter manifolds, incorrect calibration of a DP meter transmitter, DP transmitter drift etc..)

2) Physical damage or partial blockage of the DP meters primary element. (For example a buckled orifice plate, a twisted cone meter assembly, a foreign object caught in the entrance to a Venturi meter etc etc..)

6.1 Incorrect Pressure or DP Reading

Let us discuss the consequences to a DP meter if the flow was undisturbed by any physical damage to the meter but yet the flow calculations were incorrect due to a problem with a pressure port or DP meter transmitter. In such a situation we will have the following result:

$$EA_t K\sqrt{2\rho\Delta P_t} \neq EA_t K_r\sqrt{2\rho\Delta P_r} \neq AK_{PPL}\sqrt{2\rho\Delta P_{PPL}} \quad \text{--- (28)}$$

Let us denote $\dot{m}_t$ as the mass flow rate prediction when applying equation 16, $\dot{m}_r$ as the mass flow rate prediction when applying equation 17 and $\dot{m}_{PPL}$ as the mass flow rate prediction when applying equation 18. Let us consider the PLR> ½ case. If there was a low throat pressure reading (say, due to a port blockage) the result would be equation 28a, i.e. equation 28b. This is graphically illustrated in Fig. 30.

$$AK_{PPL}\sqrt{2\rho\Delta P_{PPL}} < EA_t K\sqrt{2\rho\Delta P_t} < EA_t K_r\sqrt{2\rho\Delta P_r} \text{ -- (28a) or } \dot{m}_{PPL} < \dot{m}_t < \dot{m}_r \text{ --(28b)}$$

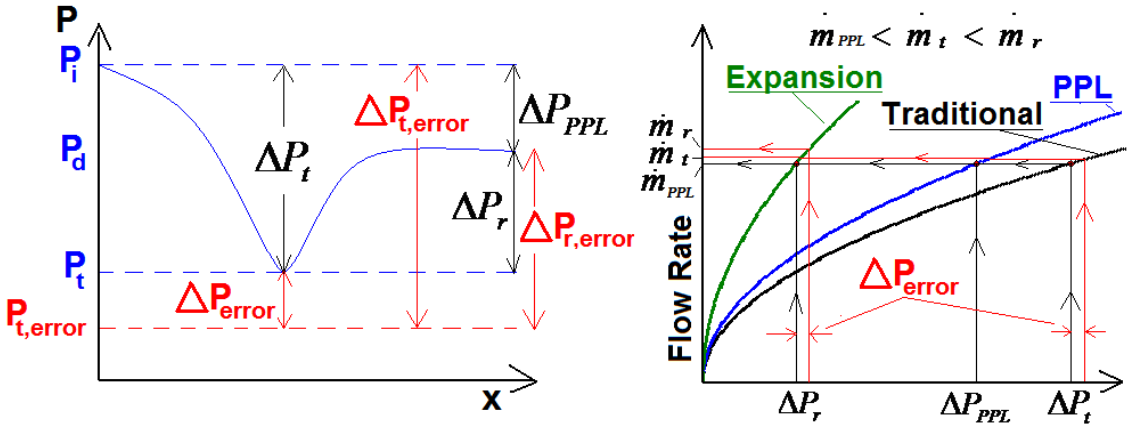

Fig 30. Graphical representation on the effect of an artificially low throat pressure.

Any one pressure port with a problem affects two of the three DP readings. Note that in this example it is the traditional and recovery DP's that have the errors. The PPL is unaffected as the measurement does not include the throat pressure tap information. Furthermore, if only the affected traditional DP and recovery DP are measured so that the PPL is found by equation 15, the errors cancels out thus making the PPL estimate still correct as the traditional DP and PPL are in error by the same magnitude as they are being caused by the same error in the low pressure port reading. Here, in this example, the errors are both positive. That is, the low throat pressure reading increases the traditional and recovered DP readings. However, note that for the different possible pressure port errors it is the modulus that must be the same not the sign. Depending on what pressure tap has what problem (i.e. an artificially high or low pressure) the DP error caused on the two DP's in question can be both positive, both negative or they can be opposites, but the magnitude of the modulus of each DP error is always equal. A negative error indicates that the pressure read is less than it should be and a positive error indicates that the pressure read is greater than it should be. For the six cases of artificially high or low pressures at each of the three different pressure ports the situation is described in Table 3.

Low Inlet Pressure Read, P_i $\dot{m}_{PPL} < \dot{m}_t < \dot{m}_r$ ΔP_t and ΔP_{PPL} are in error. $\lvert\Delta P_{t\,error}\rvert = \lvert\Delta P_{PPL_{error}}\rvert = \lvert\Delta P_{error}\rvert$ $\Delta P_{t_{error}}$ is negative , $\Delta P_{PPL_{error}}$ is negative $\frac{\Delta P_{PPL}}{\Delta P_t} < \left(\frac{\Delta P_{PPL}}{\Delta P_t}\right)_{correct}, \frac{\Delta P_r}{\Delta P_t} > \left(\frac{\Delta P_r}{\Delta P_t}\right)_{correct}$	High Inlet Pressure Read, P_i $\dot{m}_r < \dot{m}_t < \dot{m}_{PPL}$ ΔP_t and ΔP_{PPL} are in error. $\lvert\Delta P_{t\,error}\rvert = \lvert\Delta P_{PPL_{error}}\rvert = \lvert\Delta P_{error}\rvert$ $\Delta P_{t_{error}}$ is positive , $\Delta P_{PPL_{error}}$ is positive $\frac{\Delta P_{PPL}}{\Delta P_t} > \left(\frac{\Delta P_{PPL}}{\Delta P_t}\right)_{correct}, \frac{\Delta P_r}{\Delta P_t} < \left(\frac{\Delta P_r}{\Delta P_t}\right)_{correct}$
Low Throat Pressure Read, P_t $\dot{m}_{PPL} < \dot{m}_t < \dot{m}_r$ ΔP_t and ΔP_r are in error. $\lvert\Delta P_{t\,error}\rvert = \lvert\Delta P_{r_{error}}\rvert = \lvert\Delta P_{error}\rvert$ $\Delta P_{t_{error}}$ is positive , $\Delta P_{r_{error}}$ is positive $\frac{\Delta P_{PPL}}{\Delta P_t} < \left(\frac{\Delta P_{PPL}}{\Delta P_t}\right)_{correct}, \frac{\Delta P_r}{\Delta P_t} > \left(\frac{\Delta P_r}{\Delta P_t}\right)_{correct}$	High Throat Pressure Read, P_t $\dot{m}_r < \dot{m}_t < \dot{m}_{PPL}$ ΔP_t and ΔP_r are in error. $\lvert\Delta P_{t\,error}\rvert = \lvert\Delta P_{r_{error}}\rvert = \lvert\Delta P_{error}\rvert$ $\Delta P_{t_{error}}$ is negative , $\Delta P_{r_{error}}$ is negative $\frac{\Delta P_{PPL}}{\Delta P_t} > \left(\frac{\Delta P_{PPL}}{\Delta P_t}\right)_{correct}, \frac{\Delta P_r}{\Delta P_t} < \left(\frac{\Delta P_r}{\Delta P_t}\right)_{correct}$
High Downstream Pressure Read, P_d $\dot{m}_{PPL} < \dot{m}_t < \dot{m}_r$ ΔP_{PPL} and ΔP_r are in error. $\lvert\Delta P_{PPL\,error}\rvert = \lvert\Delta P_{r_{error}}\rvert = \lvert\Delta P_{error}\rvert$ $\Delta P_{PPL_{error}}$ is negative $\Delta P_{r_{error}}$ is positive $\frac{\Delta P_{PPL}}{\Delta P_t} < \left(\frac{\Delta P_{PPL}}{\Delta P_t}\right)_{correct}, \frac{\Delta P_r}{\Delta P_t} > \left(\frac{\Delta P_r}{\Delta P_t}\right)_{correct}$	Low Downstream Pressure Read, P_d $\dot{m}_r < \dot{m}_t < \dot{m}_{PPL}$ ΔP_{PPL} and ΔP_r are in error. $\lvert\Delta P_{PPL\,error}\rvert = \lvert\Delta P_{r_{error}}\rvert = \lvert\Delta P_{error}\rvert$ $\Delta P_{PPL_{error}}$ is positive , $\Delta P_{r_{error}}$ is negative $\frac{\Delta P_{PPL}}{\Delta P_t} > \left(\frac{\Delta P_{PPL}}{\Delta P_t}\right)_{correct}, \frac{\Delta P_r}{\Delta P_t} < \left(\frac{\Delta P_r}{\Delta P_t}\right)_{correct}$

Table 3. The response of generic DP meters to individual errors in pressure port readings.

Equation set 28 can indicate if there is a problem with the DP meter and set of a warning indicator even if the standard traditional DP meter equation is still giving seemingly believable results and under traditional operation there would be no sign of it being in error. If the problem is with one single pressure port the six possibilities, of artificially high or low pressures (e.g. caused by leaks, open manifold valves, hydrate, salts

or ice blockages etc.) are reduced to three as the readings $\dot{m}_{PPL} < \dot{m}_t < \dot{m}_r$ or $\dot{m}_r < \dot{m}_t < \dot{m}_{PPL}$ each indicate three of the six possible problems. Furthermore, if we find that there is no agreement between the three equations but yet the traditional meter equation 17 does not have the mid value then a problem has been found and we know it is not due to one single incorrect pressure reading at one pressure port. This problem is unspecified as it is not showing the symptoms of being caused by a single pressure port problem but crucially, a problem has been identified where it perhaps would have not been if the diagnostic system was not in use. Examples that could cause such unspecified readings are two blocked ports, damage to the primary element, one port blocked with one DP transmitter with drift, two DP transmitters with drift etc. Therefore, this diagnostic methodology is most useful for giving assurance of the health of the flow rate reading but it can give limited diagnostic information as well.

6.1.a. Worked Examples for a DP Meter with Pressure Port and / or DP Measurement Problems

	Column No.:	1	2	3	4	5
			Typical		Pt	Pd
		Precise	Real	DPt drift	-0.06%	0.01%
		Values	Values	2% low	(-2983 Pa)	(+497 Pa)
Row No.						
1	Actual Mg (kg/s)	7.000	7.000	7.000	7.000	7.000
2	Read Pi (Pa)	5000000	4995336	4995336	4995336	4995336
3	Read Pt (Pa)	4940069	4935404	4935404	4932423	4935404
4	Read Pd (Pa)	4991672	4986915	4986915	4986915	4987412
5	Read DPt (Pa)	59931	59680	58486	62913	59680
6	Pred Traditional Mg (kg/s)	7	6.99	6.92	7.17	6.99
7	%Mg Difference Actual & Trad Pred	N/A	-0.21	-1.19	2.41	-0.21
8	Calculated DPr (Pa)	51603	51259	50065	54492	51756
9	Pred Expansion Mg	7	6.97	6.89	7.19	7.00
10	%Mg Difference Actual & Exp Pred	N/A	-0.42	-1.59	2.67	0.06
11	Read DPppl (Pa)	8328	8421	8421	8421	7924
12	Pred PPL Mg (kg/s)	7	7.04	7.04	7.04	6.83
13	%Mg Difference Actual & PPL Pred	N/A	0.55	0.55	0.55	-2.46
14	%Mg Difference Trad & Expan Pred	N/A	-0.21	-0.399	0.250	0.271
15	% Mg Diff Trad & PPL Pred	N/A	0.77	1.77	-1.82	-2.25
16	%Mg Difference PPL & Expan Pred	N/A	-0.97	-2.13	2.11	2.58
17	PLR	0.1390	0.1411	0.1440	0.1339	0.1328
18	%PLR Difference Baseline & Found	N/A	1.54	3.61	-3.68	-4.46

Table 4. The 4", 0.6 Beta Ratio Venturi Meter Performance at Normal and Abnormal Operations.

Figure 13 showed the calibration of a 4", 0.6001 beta ratio Venturi meter. For this following worked example series let us consider this meter with a traditional upstream to throat DP transmitter and a PPL transmitter installed. The recovered DP is found by taking the difference between these two DP readings.

If we had a natural gas flow at 50 bara and 30 ^{0}C (giving say a 50.4 kg/m^3 density) and a flow rate of 7 kg/s, then, according to the meters calibration the performance (ignoring the calibration and instrument uncertainties) would be as shown in Table 4, column 1. In actual flow applications it should be remembered that the flow coefficients used were fitted to data sets with small but distinct scatter and therefore they are never *precisely* correct for each and every point. Furthermore, instrument readings have uncertainties. Therefore, in reality, a more realistic set of results when the meter is operating correctly is suggested in Table 4, column 2. Notice that the three flow equations (16 to 18) all predict the correct mass flow rates to within ±1% (see column 2, rows 7, 10 & 13 respectively), i.e. within each equations stated uncertainties (see Figure 13). Notice also, that the three flow equations do not agree with each other (see column 2, rows 14 to 16). However, crucially, as all three predict the actual mass flow rate to within their respective uncertainties there is not enough difference in the results to trigger a system warning. In fact the difference required between any two flow predictions before the system could produce a warning is suggested to be the root mean square (rms) of the two flow rate uncertainties. In this case it was found that (see Figure 13) the expansion meter (i.e. equation 17) had an uncertainty of 1.03% while the other two meters (i.e. equations 16 & 18) each had an uncertainty of 1%. Therefore, for example, the difference between the traditional and expansion flow meter predictions before a warning would be produced has to be in this case:

$$rms = \sqrt{(1.03)^2 + (1)^2} = 1.436\,\% \approx 1.45\,\%$$

Here then, any difference between any two predictions greater than their rms % could signal the possibility that the metering system has a problem. Also note, that the same information is contained in the raw DP readings. The PLR of this meter was found during calibration to be 0.1390 ±3%. If the PLR exceeds this ±3% variance then this (which is in fact the same information as above analysed in an alternate way) also signals the possibility that the metering system has a problem. In the case of column 2, rows 14 to 16, we see that the maximum difference in equations 16 to 18 is < ±1 and from column 2, row 18 we see the PLR value is <±3% of the calibration value. Hence the system is considered serviceable. Now let us introduce malfunctions to this correctly operating system and examine the effect on the system.

Worked Example One: A Drifting DP Transmitter

Now, let us consider a case where the DP transmitter measuring the traditional upstream to throat DP has drifted by -2%. The PPL transmitter has maintained its calibrated performance. The traditional DP which was being read as 59680 Pa (Table 4, column 2) is now being read as 58486 Pa (column 3). The PPL is still the same reading but the error in the traditional DP transmitter transfers to the recovered DP estimation. The result is shown in Table 4, column 3.

The traditional (equation 16) and expansion (equation 17) meter flow rate predictions are now outside their uncertainty claim (see column 3, rows 7 & 10). The PPL meter flow rate prediction does not use information from the traditional DP transmitter and therefore its performance is unaltered (see column 3, row 13). In a real application the actual mass flow rate is unknown so this comparison would not be possible. However, it is possible to compare the three flow predictions (equations 16 to 18) to each other. If the DP meter is operating correctly these three equations must equate to each other within the rms of the largest uncertainties. Therefore, for this example, we know from calibration of the meter in question that if the metering system is operating correctly the three flow equations can not differ by > ±1.45%. However, here we see (column 3, rows 15 & 16) that the difference between the traditional and PPL meter flow rates (equations 16 & 18) and the difference between the expansion and PPL meter flow rates (equations 17 & 18) are both > ±1.45%. Also the PLR calculated is 3.61% (i.e. column 3, row 18) and therefore out with the calibrated value by > ±3%. Hence, a diagnostic system would signal a warning that the system has a problem. It does not state *what* the problem is but crucially, unlike the traditional DP meter system, this rudimentary diagnostic methodology has warned that *something* is wrong and therefore a warning is given that the meter may not be serviceable.

Note that if the diagnostic system was not in place and this Venturi meter was being used in the traditional way, i.e. a single DP transmitter was installed between the upstream and throat pressure taps only, it is unlikely the traditional flow rate predictions error of -1.19% (column 3, row 7) caused by the transmitter drift would be noticed. However, with the use of the diagnostic system a warning is produced and the metering system would be given maintenance. Even if it then operated within the diagnostic acceptable limits but happened to be at the very limit of uncertainty for the traditional meters calibration (-1%) the meter is still 0.19% more accurate due to the maintenance initiated by the diagnostic systems warning. At this flow rate the saving of the 0.19% of gas is a saving greater than 40,000 SCFD. In the likely event the system predicted the flow rate better than -1% the saving in gas would of course be greater.

In this case it should be noted that if the DP transmitter was suspected and safety procedures allow, this DP meters traditional upstream to throat DP transmitter can be removed for servicing or replacement without taking the meter completely out of service. The metering system would continue to predict a flow rate to ±1% by use of equation 18, while the PPL transmitter is in operation.

Worked Example Two: A Problem at the Throat Pressure Port

Let us consider a case where the 4", 0.6 beta ratio Venturi meter being discussed (Figure 13) has a problem at the throat pressure tap. In this example let us say the pressure is artificially low. This scenario can occur if the port has become plugged (e.g. by hydrates, salts, ice, scale etc) at a lower pressure than the current flow conditions, etc.. The inlet pressure and PPL transmitters are unaffected by this leak. The traditional and recovery DP predictions found by information received from the correctly operating traditional DP transmitter are affected by the artificially low throat pressure. For this example say the throat pressure reading by the DP transmitters is -0.06% of the actual correct value. The traditional DP, which should be

read as 59680 Pa (Table 4, column 2) is now being read as 62913 Pa (column 4), i.e. 5.4% high. That is, the throat pressure is 3233 Pa / 13" water column low. The results are shown in Table 4, column 4.

Note the numerical results in Table 4 match the generic predictions for this condition stated in Table 3. The traditional (equation 16) and expansion (equation 17) meter flow rate predictions are outside their uncertainty claim (see column 4, rows 7 & 10). The PPL meter flow rate prediction does not use information from the throat pressure port and therefore its performance is unaltered (see column 4, row 13). Again, in a real application the actual mass flow rate is unknown so this comparison would not be possible. However, comparing the three flow predictions (equations 16 to 18) to each other shows that the two of the three comparisons do not equate to each other within the rms of their respective uncertainties. That is, column 4, rows 15 & 16 show that the difference between the traditional and PPL meter flow rates (equations 16 & 18) and the difference between the expansion and PPL meter flow rates (equations 17 & 18) are both > ±1.45%. Also the PLR calculated is -3.68% (column 4, row 18) and therefore out with the calibrated value by > ±3%. Hence, again the diagnostic system could signal a malfunction warning.

Note that if the diagnostic system was not in place and this Venturi meter was being used in the traditional way, it is unlikely the traditional flow rate predictions error of +2.41% (column 4, row 7) would be noticed. However, if the error is found due to the diagnostic method and the meter then operates correctly even at the acceptable limit of +1% the meter is still 1.41% more accurate due to the maintenance initiated by the diagnostic systems warning. At this flow rate the gas prediction accuracy improves by at least 2.4e5 SCFD.

Worked Example Three: A Problem at the Downstream Pressure Port

The more sophisticated a system the more opportunity there is for it to malfunction. There is a chance the downstream pressure port will become blocked instead of the inlet or throat pressure tap. Let us consider the case where the same meter set up has a blocked downstream tap, causing an artificially higher downstream pressure (say + 0.01%). The PPL read when the system is operating correctly is 8421 Pa (Table 4, column 2, row 11) but now the PPL read is 7924 Pa (column 5, row 11). The traditional DP reading is not affected. The recovered DP is affected. The flow prediction results are shown in Table 4, column 5.

Note the numerical results in Table 4 match the generic predictions for this condition stated in Table 3. The PPL (equation 18) meter flow rate prediction is outside the meters uncertainty claim (see column 5, row 13). For *this* DP meter with this example the pressure difference between the actual and read downstream pressure is not great enough for the expansion meter (equation 17) to predict outside its stated uncertainty (see column 5, row 10). The traditional meter flow rate prediction (equation 16) does not use information from the downstream pressure port and therefore its performance is unaltered (see column 5, row 7). Again, in a real application the actual mass flow rate is unknown so this comparison would not be possible. However, comparing the three flow predictions (equations 16 to 18) to each other shows that not all the equations equate to each other within the rms of their respective uncertainties. That is, column 5, rows 15 & 16 show that the difference between the traditional and PPL meter flow rates (equations 16 & 18) and the difference between the expansion and PPL meter flow rates (equations 17 & 18) are both > ±1.45%. Also the PLR calculated is -4.46% (column 5, row 18) and therefore out with the calibrated value by > ±3%. Hence, again the diagnostic system would signal a warning that the system has a problem.

In this situation the meter maintenance would find the problem was with the downstream port and that the primary flow rate calculation (equation 16) was therefore giving the correct flow rate (within its stated uncertainties). Nevertheless, this situation is viewed by the author to be better than blindly hoping the DP meter is working correctly. Furthermore, a blockage of any pressure port signals that the meter is encountering adverse conditions. If one pressure port is blocked then it is common for the same blockage phenomena to then go on to block the other ports in due time. This diagnostic methodology gives a warning of such a problem as it begins.

6.2. Worked Examples of DP Meters with Damage or Foreign Objects Trapped at the Primary Element

6.2.a Beveled Trailing Edge Orifice Plate Meter Abnormal Operations

Plates have operational issues that affect performance, e.g. backward installed plates, plastically deformed plates, i.e. "buckled" / "warped" / "bent" plates, (Figure 33a), worn edges (Figure 33b), contamination etc.. Examples of literature discussing orifice meter errors due to abnormal operation include discussions by ISO

[10] and GRI [11], as well as technical papers by Pritchard et al [12] and Brown et al [13]. These documents discuss the affect on the meter of the abnormality and some attempt to quantify the resulting error and offer correction factors to back calculate actual flow rates after the event. Brown et al [13] do mention the change in PPL recorded before and after a plate was incorrectly installed, but this information was only utilized in an (excellent) attempt to derive the resulting discharge coefficient. The common trait in the literature is one of attempting to quantify the error after it has been discovered by some external event (such as periodic mass balance, scheduled maintenance etc.). There is little on how to let the DP meter system itself diagnose a problem from the moment it occurs. Such a diagnostic system would allow the problem to be immediately fixed thus reducing the requirement for corrective calculations. That is, prevention is better than cure. Let us look at the effects of some non-standard plate conditions on equations (16 to 18) and PLR values, in order to ascertain if there is any potential for diagnostics to be developed.

Four 4.026", 0.4967 beta ratio orifice plates with flange taps (at top dead centre) were tested at CEESI. The downstream port was at 6D from the plates. All three DP's were individually read by DP transmitters within their turndown range. A baseline was required to compare the adverse condition tests. One plate was tested with two pressures (14 Bara & 30 Bara) across a combined Reynolds number range of 308,200 to 2,090,700 (i.e. a 6.8:1 turndown). The discharge coefficient calibration was very slightly below the RHG equation predictions uncertainty band. A second plate was therefore tested at the low pressure value. This data fell in the lower half of the RHG prediction uncertainty band. Both test procedures were reviewed and found to be sound. However, the ISO data for 4", 0.5 beta ratio orifice meters appeared to be mainly for water flows (with no compressibility) and the maximum Reynolds number was < 1 million. Furthermore, the CEESI result includes the expansibility uncertainty, higher Reynolds numbers and the particular reference meter used had an uncertainty of ±0.53%. This is enough to explain the very slight differences between the RHG prediction and the data. The difference is also an order of magnitude less than is required to affect the purpose of these tests. For that reason the discharge coefficient was set at 0.6 (±0.4%). Figure 31 shows the ISO RHG and CEESI data comparison.

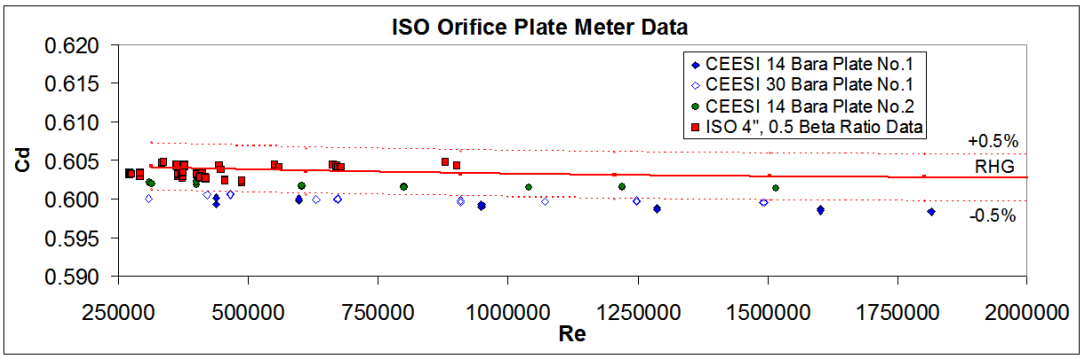

Fig 31. RHG Prediction & CEESI 4", 0.5 Beta Ratio Data Results

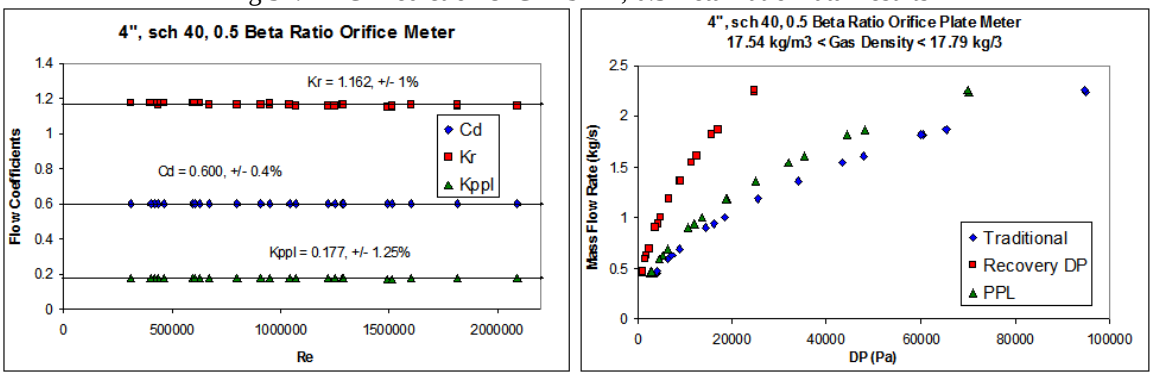

Fig 32. CEESI 4", Sch 40, 0.5 Beta Ratio Orifice Plate Meter Air Blow Down Base Line Test.

Figure 32 shows the standard operation results. As expected, the results are similar to the earlier 4", 0.5 beta ratio orifice meter data (see Figure 9). The PLR was 0.735 ±0.6%. The PRT diagram behaves like Figure 5b. As the discharge coefficient was fitted to ±0.4%, the expansion flow coefficient to ±1% and PPL

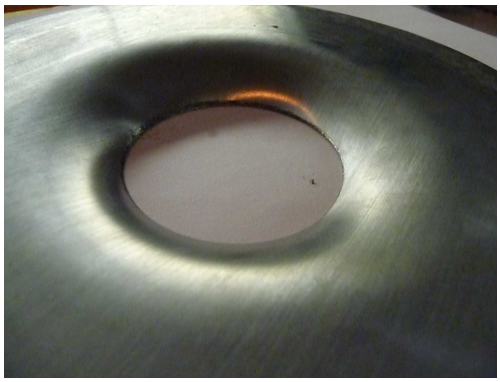

Fig 33a. Buckled Plate (sharp edge upstream)

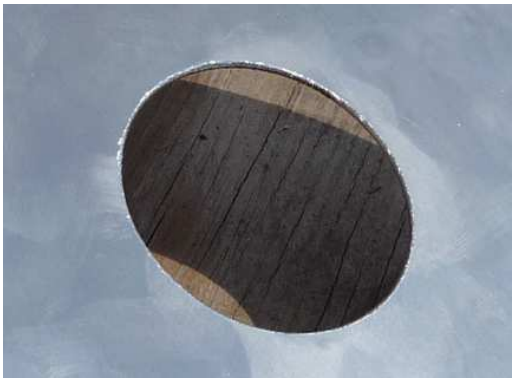

Fig 33b. Sharpness of Orifice Inlet Worn Down.

	Backward	Buckled	Blunt Edge
	Plate % Error	Plate % Error	Plate % Error
Equation 16	-15.43	-29.49	-8.27
Equation 17	-10.14	-19.53	-5.27
Equation 18	-17.79	-33.80	-9.76

Table 5. The Performance of the Three Flow Equations with the Non-Standard Plate Conditions.

	Max Norm	Backward	Buckled	Blunt Edge
	% rms	Plate % Error	Plate % Error	Plate % Error
% diff Equ. 16 & 18	1.31	-2.79	-6.10	-1.63
% diff Equ. 16 & 17	1.08	6.25	14.12	3.26
% diff Equ. 17 & 18	1.60	-8.51	-17.73	-4.73
	Max Norm ±%			
PLR	±0.6	-4.86	-11.07	-2.44

Table 6. The Three Flow Rate Predictions Inter-Comparisons.

coefficient to ±1.25% (all at 95% confidence), the maximum difference required between any two flow predictions to set off an alarm is the % rms of the two largest uncertainties:

$$rms = \sqrt{(1)^2 + (1.25)^2} \approx 1.6\,\%$$

The baseline test matrix was repeated for non-standard cases. Figures 34 to 36 and Tables 5 & 6 show the results for the plate installed backwards, the buckled plate and the blunt edge orifice plate scenarios. In all cases, when used traditionally, we see that the non-standard conditions have caused the meter to predict the flow rate out with the stated uncertainty (±0.4%). Traditionally there would be no diagnostic ability to indicate a problem as in operation the actual flow rate is unknown so the values in Table 5 are unknown. The flow rate predicted by equation 16 (see Table 5) would be accepted unless information external to the flow meter was available and checked to show some discrepancy. Also note that in all non-standard conditions equations 17 & 18 also failed to give the correct flow rates. However, it is significant that equations 17 & 18 gave ***different*** erroneous flow rates. Under correct operation each of the three DP meter flow equations will individually give the correct flow rate to within their relatively small uncertainty bands. These *differences* between the predictions are known. Figures 34 to 36 and Table 6 show these results. The maximum percentage difference between any two predictions for standard conditions is shown in Table 6, column 1. The backwards installed plate, the buckled plate and the blunt edge plate all have differences between the flow rate predictions well in excess of the maximum allowed for standard conditions thereby indicating a problem. As a consequence, one diagnostic check must be that all three equations agree. Also note that Table 6 shows the difference between the set standard condition PLR of 0.735 and the actual values found during the non-standard tests. With the baseline tests showing a PLR uncertainty of ±0.6% all abnormal conditions tested show a clear discrepancy. Therefore a result showing flow rate prediction and / or PLR discrepancies signals that ***something is wrong*** and the meter may not be serviceable.

6.2.b Partial Blockage at the Throat of a Cone Meter

The primary element of a DP meter is intrusive to the flow. Unfortunately, many flows are not clean. Solid objects can be found inside pipe flows, e.g. rock fragments from hydrocarbon reservoirs, debris from failed

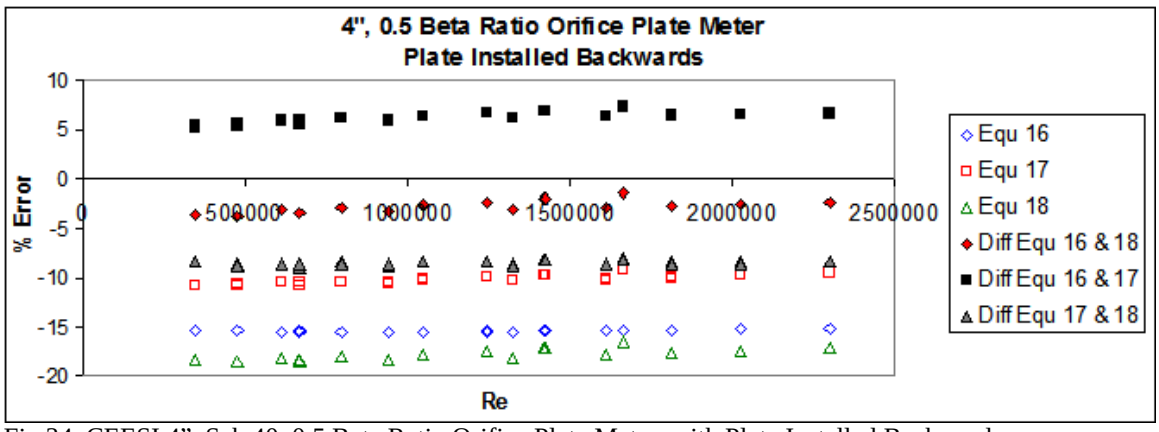

Fig 34. CEESI 4", Sch 40, 0.5 Beta Ratio Orifice Plate Meter with Plate Installed Backwards.

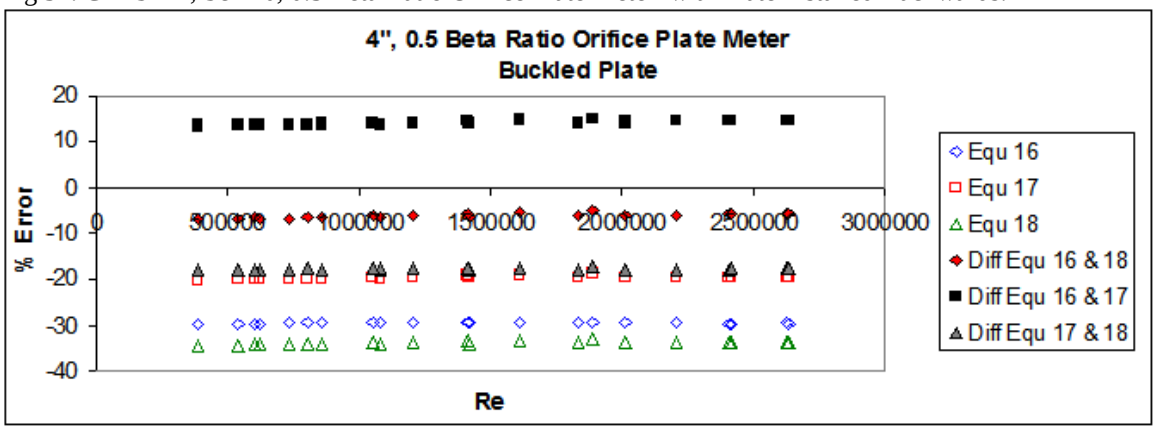

Fig 35. CEESI 4", Sch 40, 0.5 Beta Ratio Orifice Plate Meter with a Buckled Plate.

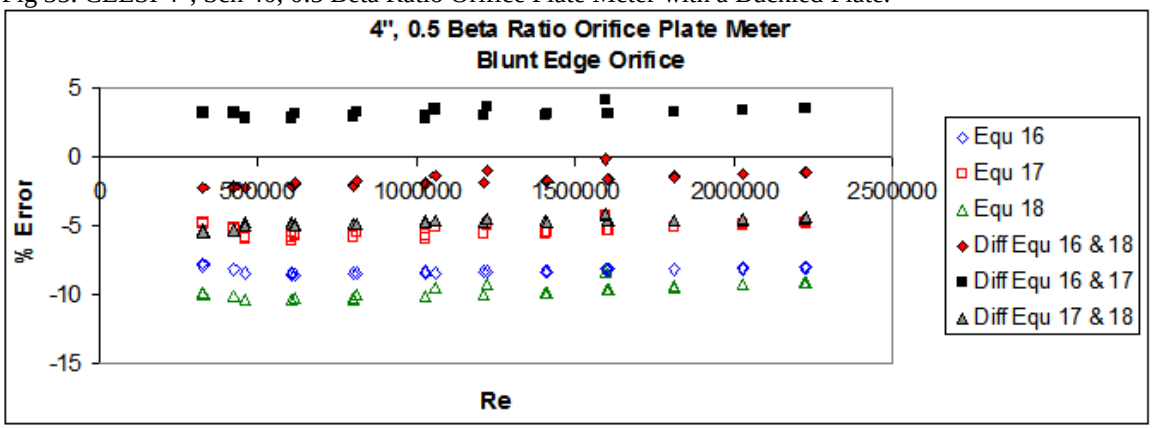

Fig 36. CEESI 4", Sch 40, 0.5 Beta Ratio Orifice Plate Meter with a Blunt Edge.

upstream components, welding rods, bolts and any other material can be accidentally left in the pipe during set up etc. Objects can therefore get trapped at the primary element. This effectively changes the primary element geometry and therefore the characteristics of the DP meter. Foreign objects trapped at a primary element can cause significant metering errors.

Figure 16 showed the base line performance of a 4", 0.7499 beta ratio cone DP meter. To discuss the issue of foreign objects being trapped by a primary element and the potential for a diagnostic alarm if this was to cause a significant flow metering error, a bolt was inserted upstream of this meters cone. This was considered a realistic scenario. Figure 37a shows the test set up. (Note that all three differential pressures are being measured directly.) The flow is left to right. Figure 37b shows a picture of the inserted bolt. (It is covered in tape to reduce the potential damage caused by the lose bolt to the meters wetted surfaces.)

Fig 37a. Cone DP Meter Test Set Up

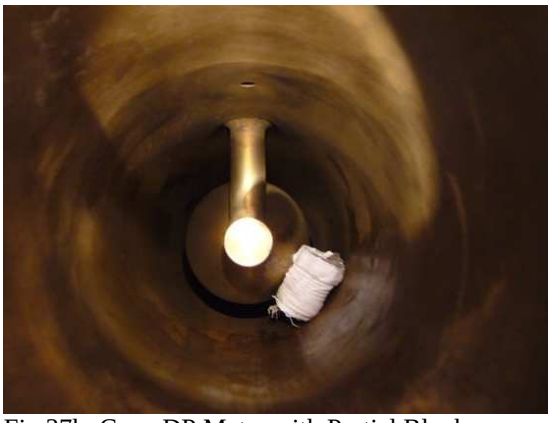

Fig 37b. Cone DP Meter with Partial Blockage

	Cone DP Meter		Max Norm	Cone DP Meter
	Trapped Bolt Av. % Error		% rms	Trapped Bolt Av. % Error
Equation 16	+15.33	% diff Equ. 16 & 18	±0.57	-5.16
Equation 17	+22.67	% diff Equ. 16 & 17	±0.64	+6.36
Equation 18	+9.38	% diff Equ. 17 & 18	±0.64	-10.84
				Trapped Bolt PLR % Error
		% diff PLR	±0.30	-10.4

Table 7. Performance of 4”, 0.7499 Beta Ratio Cone DP Meter with Trapped Bolt.

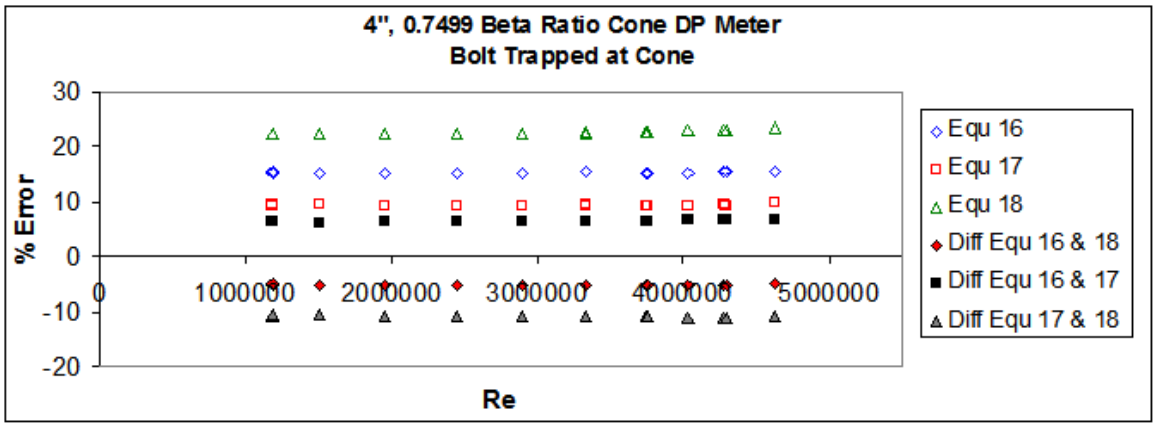

Fig 38. 4”, 0.7499 Beta Ratio Cone DP Meter with Bolt Lodged at Cone Element.

The baseline PLR was 0.564 ±0.3%. The discharge coefficient was fitted to ±0.4%, the expansion flow coefficient to ±0.5% and PPL coefficient to ±0.4% (all at 95% confidence). Therefore the minimum difference required between any two flow predictions to set off an alarm is the % rms of the two uncertainties as shown in Table 7.

This baseline tests were repeated for the non-standard case. Figure 38 and Tables 7 show the results. When used traditionally, the non-standard condition has caused the meter to predict a flow rate >15% too high. Traditionally there would be no diagnostic ability to indicate a problem. The erroneous flow rate predicted by equation 16 (see Table 7) would be accepted unless information external to the meter was available and checked to show some discrepancy. Equations 17 & 18 also failed to give the correct flow rates. However, as previously seen with the abnormal operation orifice plate meter data sets equations 16, 17 & 18 gave ***different*** erroneous flow rates. As correct operation of the metering system has each of the three flow equations individually giving the correct flow rate to within their relatively small uncertainty bands, a consequence is that one diagnostic check must be that all three equations agree. A result showing a flow rate prediction discrepancy between the flow rate equations signals that ***something is wrong*** and the flow meter is not serviceable. Alternatively, note that Table 7 shows the difference between the set standard condition PLR of 0.564 and the actual value found during the non-standard test. With a PLR standard

condition uncertainty of ±0.3% the fact that the PLR is out by -10.4% clearly indicates a problem thereby also suggesting the flow meter is not serviceable.

7. DP Meter Diagnostic Sensitivity Issues

The sensitivity and limitations of such a DP meter diagnostic system depends on several factors. One major factor is the uncertainty of each of the baseline flow rate equations (or the percentage variation of the PLR). The more precise each of the three equations 16 to 18 the more resolution there is to see small problems. It should be remembered that the above examples were kept simple by always using constant expansion and PPL flow coefficient terms. If a meter had expansibility terms for all three flow rate equations and each flow coefficient was fitted to the Reynolds number then the accuracy of each equation would improve and with it the resolution of the DP meter diagnostic system (i.e. smaller errors could be seen).

This diagnostic methodology is wholly based on comparisons of three DP's. DP's are measured by DP transmitters with set ranges. Like all instrumentation, the smaller the property being measured, the more difficult the measurement becomes. The uncertainty increases for any instrument as the measured value diminishes. Therefore, for a given DP meter, the lower the flow rate (for otherwise set conditions) the lower all three DP's become and the larger the uncertainty there is on each DP measurement. As the diagnostic capability requires as good a DP measurement as possible the ability of the DP meter to diagnose a problem is enhanced by higher flow rates and degraded by lower flow rates. Thankfully for industry the higher the flow rate the more important it is to diagnose incorrect flow measurement.

A related subject to the DP transmitter uncertainty issue is the issue of, for any flow rate and PLR values the smaller the flow rate prediction error (i.e. the lighter the meter damage, or the smaller the impulse line leak, or the smaller the blockage at the primary element etc. etc.) the more the resolution required between the DP's (and therefore the flow rate equations) to pick up the problem. Figure 39 shows a sketch of the typical situation if the flow rate is low and / or the malfunction of the meter is relatively small.

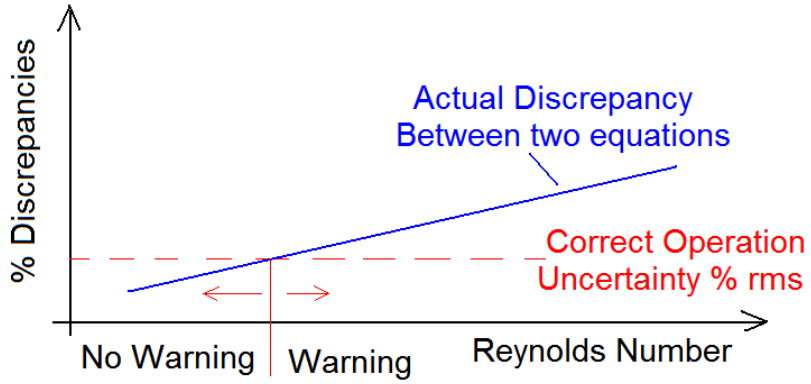

Fig. 39. Sketch of the DP Diagnostic Methodologies Sensitivity to Reynolds Number

Initial evidence suggests that the methodology can be rather sensitive to a pressure tap problem or DP transmitter errors as at least one DP transmitter stays reading the correct flow rate while the other diverges away from it. The case of the damaged meters is slightly different. Here the flow meter characteristics have been changed and therefore all the readings are incorrect. A review of Figures 34, 35, 36 & 38 shows that all three equations have errors that tend in the same direction. This could mean it takes a greater error than for the pressure tap problem or DP transmitter error problem for the difference in the equations to become apparent. However, it can be seen by the above examples there is still easily enough resolution for the diagnostic methodology to be of value to industry.

8. Conclusions

DP meters are relatively inexpensive, sturdy, reliable, well understood and trusted flow meters. However, most engineers do not associate this flow meter type with having any inherent diagnostic capabilities. It has been shown here that by considering the well understood fluid mechanics phenomena through out the entire meter body there is potential for the generic DP meter design to be further developed. This development would create redundancy factors, and through them a diagnostic capability could be developed which could identify meter malfunction in many common adverse conditions where currently DP meter users have no

way of knowing the meter is unserviceable without using evidence external to the metering system. This rudimentary diagnostic capability would be easily understood from first principles and from the evidence of the multiple data sets investigated so far this generic DP meter diagnostic capability is relatively simple, powerful and reliable. Therefore, by applying this diagnostic methodology flow meter users would have greater assurance that the flow rates are correct.

Appendix: Rules regarding the magnitude of the flow coefficients K, K_r, K_{PPL}

Consideration of the flow phenomena through any DP meter indicates that the flow meter has a discharge coefficient, expansibility and therefore a flow coefficient less than unity. (Some Venturi meters have discharge coefficients slightly greater than unity but this is known to be due to pressure tap imperfection effects.) In order to discuss how the expansion flow coefficient magnitude is affected by this same phenomena it is first necessary to show the reasoning why the flow coefficient, K, is always less than unity.

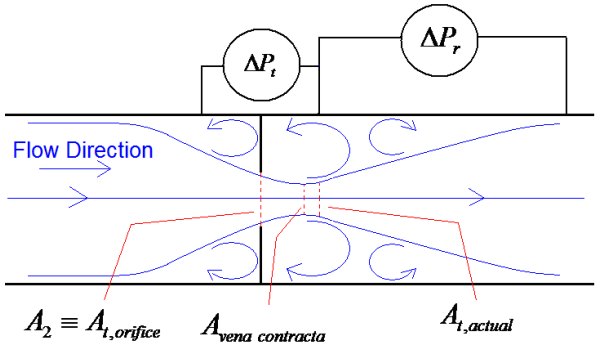

Fig A1. Sketch of Typical Flow Through an Orifice Plate Flow Meter.

In an ideal DP meter system the flow is reversible, incompressible and the geometric minimum cross sectional area (or "throat" area) is where the low pressure is located and read from. In this ideal situation equation 5 is applicable. In reality this ideal world does not exist. Two correction factors account for real world imperfections, i.e. the density correction (called the "expansibility") and the discharge coefficient, which accounts for effects such as energy loss and the fact that often DP meter designs have a throat area used in the flow equation that is not the actual cross sectional flow area where the low pressure is read.

For liquid flows the density remains constant and the expansion factor is unity. For gas flows the DP from high to low pressure ports reduces the density and hence the expansibility is less than unity to correct for the use of the higher inlet density value. The DP between these pressure ports is caused in reality by both momentum changes and friction. Equation 5 only accounts for the momentum changes. As pressure change due to friction is inevitable and always a loss (i.e. unrecoverable) the actual traditional DP read is always greater than if the friction pressure loss did not exist. Therefore the component of the correction factor that accounts for the effect of friction must reduce the equations flow rate prediction. Furthermore, in many DP meter designs the flow passes through the geometric throat area and continues expanding in fluid mechanic terms down to a smaller cross sectional area downstream (called a "vena contracta") before it begins to compress as it geometrically expands back to the pipe area. Figure A1 indicates this for an orifice meter. The DP meter equation 5 uses the geometric throat area. However, this is not always the true flow cross sectional area at the location where the low pressure is read. Typically, the low pressure port of a DP meter is located in the vicinity of the vena contracta. However, the vena contracta position is known to vary slightly with flow conditions. Hence there is no such place as an ideal low pressure port location. Therefore, it is convention to use the known throat area and add a correction imbedded in the discharge coefficient. In virtually all real cases the low pressure port is close enough to the vena contracta so that the actual geometric cross sectional area is less than the throat area being used in equation 5. That is, a correction factor would reduce this area size from that of the throat area to the actual area. The result is that all three of these factors, i.e. expansibility, friction effects and throat area error, indicate that their individual effect is to make equation 5 over predict the flow rate. Hence *the product of the expansibility and discharge coefficient, i.e., the flow coefficient, must be less than unity*. That is:

$$\dot{m} = EA_t \varepsilon C_d \sqrt{2\rho(P_i - P_t)} = EA_t K \sqrt{2\rho \Delta P_t} \quad \text{--- (16) where} \quad \varepsilon < 1,\ C_d < 1\ \&\ K = \varepsilon C_d < 1$$

Equation 6 was derived with the same assumptions as equation 5. For a stand alone geometric expansion meter the inlet gas flow will compress as it flows through the meter meaning that a "compression" factor is required. In reality the compression factor for liquid flows is unity and greater than unity for gas flows. If the expansion meter in question is the throat to downstream of a standard DP meter, where the "inlet" density being used in equation 17 is not the throat density but the meter body inlet density, the actual gas density through the expansion meter will always be less than the density being used and so an expansibility term would be required. In this case, i.e. the case this paper is discussing, the expansion DP meter has its own expansibility factor which is less than unity.

The geometric expansion meter has the same issue as the traditional geometric converging meter, with the low pressure being measured at the same flow cross sectional area. Hence, this actual cross sectional area is less than the throat area being used in the flow equation 17 and a correction factor is required. It must be less than unity. Again the DP between the pressure ports is caused in reality by momentum changes and friction. Equation 6 only accounts for the momentum change. As pressure change due to friction is inevitable and always a loss the actual DP recovered is always less than if there was no friction. Therefore, a correction factor greater than unity is required to remove the friction effect. (This is the crucial difference between the flow coefficient and expansion flow coefficient.) The expansion meter imbedded in the traditional DP meter body has an expansion flow coefficient that incorporates the expansibility, the friction effect and area error issues. However, unlike the traditional meter, not all these factors are less than unity. The friction / energy loss factor is greater than unity. It is therefore not the case that the expansion flow coefficient must be less than unity. Depending on primary element design the friction effect or the throat area correction can dominate and hence *the expansion flow coefficient can be greater **or** less than unity*.

Finally, note the quantity of the PPL across any given DP meter depends on flow conditions and primary element design. Hence the PPL can be greater or less than the flows gas dynamic pressure, i.e. the minor loss coefficient, and therefore the PPL coefficient, can be greater or less than unity.

References

1. Fox & McDonald, "Introduction to Fluid Mechanics, Ed. 3", John Wiley & Sons, 1985.
2. Steven. R., "Wet Gas Metering", Strathclyde University PhD Thesis, 2001.
3. Munson, Young & Okiishi, "Fundamentals of Fluid Mechanics", 5th Edition, ISBN 0-471-67582-2, John Wiley & Sons, Inc.
4. Miller R., "Flow Measurement Engineering Handbook", 3rd Ed. McGraw Hill, ISBN 0-07-042366-0
5. International Standard Organisation, "Measurement of Fluid Flow by Means of Pressure Differential Devices, Inserted in circular cross section conduits running full", no. 5167, Part 4.
6. Kegel T., "Uncertainty Analysis of a Wet Gas Test Facility", 4th North American Conference on Multiphase Technology, Banff, Canada, 3rd-4th June, 2004.
7. Geach D. & Jamieson A., "Wet Gas Measurement in the Southern North Sea", North Sea Flow Measurement Workshop, Tonsberg, 18th-21st October 2005.
8. Peters R., Steven R., George D., Bowles E. & Nored M., "Tests on the V-Cone Flow Meter at South West Research Institute and the Utah State University in Accordance with the New API Chapter 5.7 Test Protocol", North Sea Flow Measurement Workshop, St Andrews, UK, 2004.
9. De Leeuw R, "Liquid Correction of Venturi Meter Readings in Wet Gas Flow", North Sea Flow Measurement Workshop, 1997.
10. ISO TR 12767:1998. Measurement of Fluid Flow by Means of Pressure Differential Devices – Guidelines to the Effect of Departure from the Specifications and Operating Conditions given in ISO 5167.
11. GRI Report No. 01/0074, South West Research Institute Project No. 18-8890, "Orifice Meter Operational Effects – Orifice Meter Calibration for Backwards - Facing Orifice Plates".
12. Pritchard M., Marshall D. & Wilson J., "An Assessment of the Impact of Contamination on Orifice Plate Metering Accuracy", North Sea Flow Measurement Workshop, St Andrews, UK, 2004.
13. Brown G., Reader-Harris M., Gibson J., Stobie G. "Correction of Readings from an Orifice Plate Installed in Reverse Orientation", North Sea Flow Measurement Workshop, Glen Eagles, UK, 2000.